Microearthquake Waveforms Recorded at Tottori Microearthquake Observatory and Their Relation to Hypocentral Distributions and the Upper-Crustal Structure

By Tameshige TSUKUDA

Reprinted from the Bulletin of the Disaster Prevention Research Institute,
Kyoto University
Voume 26, March, 1976

Microearthquake Waveforms Recorded at Tottori Microearthquake Observatory and Their Relation to Hypocentral Distributions and the Upper-Crustal Structure

By Tameshige TSUKUDA

(Manuscript received March, 1, 1976)

Abstract

The microearthquake waveforms recorded at the Tottori Microearthquake Observatory (TTT) during the period from Aug., 1971 to Dec., 1975 are investigated in relation to source regions, focal depths and the upper-crustal structure. Representative waveforms which originated in respective regions in and around Tottori city, western Honshu, Japan are presented in this paper. By using P and $S-P$ times from TTT and its satellite stations we obtained locations of hypocenters, V_p/V_s values and P velocities of the crust.

Some prominent phases which appear on the seismograms are interpreted as reflected waves such as SxS and SxP, which can be estimated to be reflected at the Conrad discontinuity. Waveforms of shallow events are considerably complicated. The phases which appear between P and S waves on the seismograms of shallow events are interpreted as SP waves and channel waves of SP type propagated through the superficial layer.

Travel times of P waves and SxS waves reveal that the crustal structure beneath the Tottori area is slightly different from the model derived by the Kurayoshi and Hanabusa explosions.

1. Introduction

Seismic waves of microearthquakes occurring in the crust are largely affected by the local fine structures of the crust. Direct P and S waves are followed by various later arrivals, which would be generated in certain inhomogeneous regions of the crust and at the ground surface. It is often found that the waveforms of the microearthquakes, which occur in the same confined region are quite similar to one another. This suggests that the outline of the waveform depends largely on the seismic-wave path and most of the prominent phases which appear on microearthquake seismograms could be explained if the crustal structure were completely revealed. The purpose of this paper is to present the observational evidences of the effects of the crustal structure and the ground surface on microearthquake waveforms by using seismograms recorded at Tottori Microearthquake Observatory, Disaster Prevention Research Institute, Kyoto University.

Utilizing the data from the observation network of the Tottori Microearthquake Observatory, many researchers[1),2),3),4),5),6),7),8),9),10),11)] have investigated the microseismicities, crustal structures, earthquake generating stresses etc. . Nishida et al.[12)] and Tsukuda et al.[13)] discussed the recent tendency of the seismic activity in and around the Tottori area.

According to the above researches, a microseismically active area extends linearly

eastward, westward and southward centering around Tottori city. As the approaching directions of seismic waves of a considerable number of microearthquakes observed at Tottori station (Tottori Microearthquake Observatory) can be regarded as being nearly east, west or south, the radial and transversal components of a seismic wave can be easily discriminated on the E–W and N–S component seismograms.

The east-west trending seismic zone is the aftershock area of the Tottori earthquake of 1943 (M7.4) and its eastward and westward extensions. It covers the Hamasaka, Tottori, Yoshioka, Shikano, Misasa and Kurayoshi regions (See Fig. 1). Yoshioka and Shikano are famous for the Yoshioka and Shikano faults generated by the Tottori earthquake above mentioned. Tsukuda et al.[13] found that the distribution of epicenters and focal depths in the above seismic zone coincides well with that of the aftershocks of the earthquake of 1943.[14] Hypocenters are shallow (3–8 km) in the Tottori and Misasa regions and deep (10–15 km) in the Shikano region. In the Hamasaka region also very shallow focused events have been observed, as will be discussed in later sections.

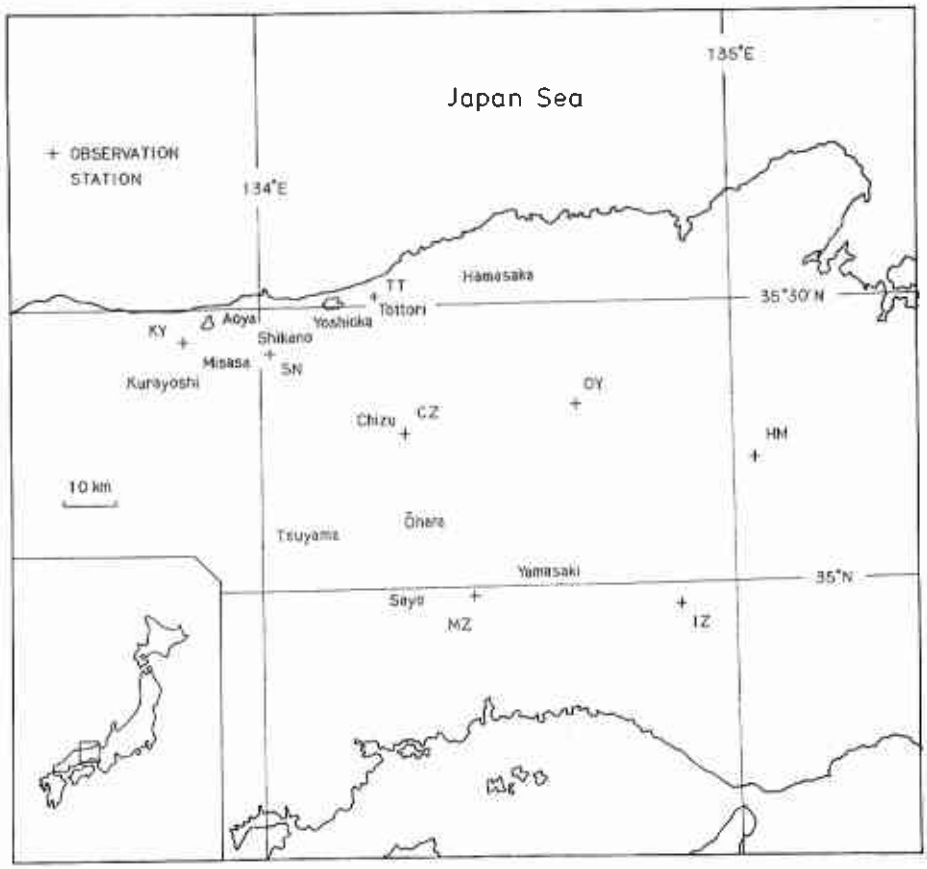

Fig. 1. Observation stations and the regions concerned.

Another seismically active area around Tottori extends along the Yamasaki fault and its north-westward extention. The Chizu, Ohara, Yamasaki and Sayo regions are included in this area (See Fig. 1). The hypocentral distribution of this area will be described in Section 4.

Prior to entering into discussions about waveforms we will examine the locations of hypocenters in the above regions and the P and S wave velocities of the crust surrounding the focal regions. A simplified method for hypocenter determination presented in Appendix 1 is used in Section 4. By the use of this method we will also discuss the P wave velocity structures. As for S wave structures we will show the results of the V_p/V_s (the ratio of P to S velocities) analysis. The list of the events used for hypocenter location and V_p/V_s is presented in Appendix 2. In addition to microearthquakes, data from quarry blasts are used for deriving crustal structure.

The waveforms of microearthquakes are so complicated that we can only concentrate on the analysis of such prominent phases as initial motions, S waves, and several later arrivals. With regard to initial P waves we especially treat angles of incidence, which would inform the velocity just below the station. The polarization directions of motion are very useful for interpreting such phases as P, SV and SH waves. The interpretation of prominent late arrivals is done in terms of the crustal structure discussed in the first half of this paper.

2. Observation stations and data

The coordinates of the stations and observation periods are listed in Table 1 and their locations together with the regions concerned are shown in Fig. 1. The western part of the network was recently established and has enabled us to investigate in detail the microseismicity in the Tottori area.

The system of the instruments installed at each station is almost the same as described by Hashizume.[3] Pen writing drum recorders with a paper speed of 4 mm/sec are operated at each station. The velocity sensitivity is 400 μkine/cm in the frequency range from 1 to 30 Hz on a seismogram paper. Every hour's radio time of NHK (Japan Broadcasting Corporation) as well as the clock time in every

Table 1. Coordinates of the observation stations together with the observation periods

Station	Code	Longitude	Latitude	X(km)	Y(km)	Altitude (m)	Period
Tottori	TT(T)	134°14′16.0″	35°30′52.9″	0.0	0.0	10	Aug. 1971–
Chizu	CZ(T)	134°17′36.8″	35°16′10.1″	5.08	−27.21	300	Sep. 1971–
Shikano	SN(T)	134°01′13.3″	35°24′37.8″	−19.75	−11.54	200	Apr. 1975–
Kurayoshi	KY(T)	133°50′01.9″	35°26′21.2″	−36.68	−8.30	100	Sep. 1972–
Mikazuki	MZ(T)	134°26′40.5″	34°59′12.0″	18.73	−58.61	200	Aug. 1964–
Oya	OY(T)	134°39′56.8″	35°19′18.5″	38.77	−21.21	230	Nov. 1969–
Izumi	IZ(T)	134°53′15.5″	34°58′20.0″	59.19	−60.15	230	Jun. 1965–
Hikami	HM(T)	135°02′36.6″	35°13′35.5″	73.27	−31.87	250	Aug. 1964–

second are also recorded on the seismogram, providing correction times.

The reading error of the correction time and time of initial onset is within a limit of 0.05 sec or so in ordinary cases, and therefore the resultant accuracy of readings for P times is 0.1 sec or so. But, strictly speaking, the accuracy depends on the ground noise of the site at the recording time.

The transducers of each station are installed on a bedrock and the ground noise level does not exceed 20–30 μkine peak to peak in ordinary times except for TT and KY where the level of traffic noises are very high in the daytime. KY particularly suffers from such noises.

TT is the only station equipped with seismographs of three components; i.e., a vertical and two horizontal ones. At SN, CZ, IZ and HM only a vertical seismograph is installed, and other stations (KY, MZ, OY) have a vertical and a horizontal one.

The Tottori station is not only favorable for the detection of microearthquakes occurring in the seismic zone around Tottori as previously mentioned, but also excellent in the maintenance of the instruments because this station is located at the Tottori Microearthquake Observatory. Therefore the earthquake table of this station can be used as a reference. All of the events analyzed in this paper have been detected at Tottori station. Moreover the seismograms shown in later sections are all those of Tottori station.

At TT about 600 or more microearthquakes (S–P time$\leq$20 sec) are registered every year. About a half of them are nearby earthquakes with S–P times less than 4–5 seconds.

In the present study we will analyse as many events as possible. But data with considerablly low quality are rejected. In the hypocenter and V_p/V_s determination we use the P and S time data with high accuracy at each station. All the data thus selected are listed in Table 6, which is presented in Appendix 2.

Most of the P and S times at MZ, OY and IZ were primarily based on the list of hypocenters compiled by Oike[11]. But some corrections were made when necessary. Those of other stations were compiled by the author.

3. Crustal structure derived by the Kurayoshi and Hanabusa explosions

The crustal structure in the Tottori area was previously derived by using data of the first and second Kurayoshi and the Hanabusa explosions[15),16)], whose profile passes through the Kurayoshi, Misasa, Shikano, Chizu regions and the vicinity of Oya station. Along the above profile the travel time curve indicates the apparent velocity, 6.05 km/s, and the layered model given in the right hand side of Fig. 2 is derived. The velocity 6.05 km/s is also comfirmed by use of the data of quarry blasts, which will be discussed in Section 5.

As will be also derived from the quarry blasts, the velocity structure is more complicated in reality. However, a simple model is useful in its own way as a tool for analyses.

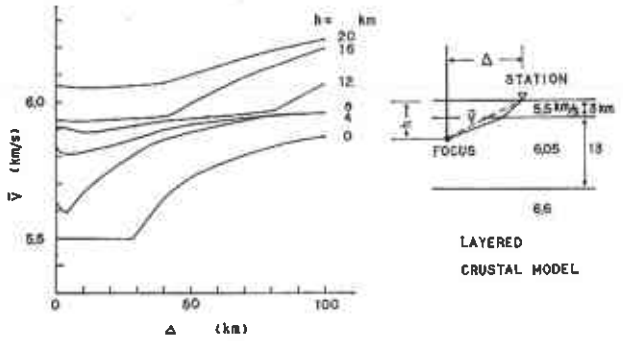

Fig. 2. Crustal Structure model and the average velocity $\bar{V}$ which is defined to be the distance from focus to station devided by the calculated travel time derived by the structure model.

The most simplified model of the structure is a homogeneous half space with a constant velocity. The microearthquakes studied in this paper are estimated to occur in the upper part of the crust, and therefore the homogeneous crustal model used instead of a layered one is sufficient for hypocenter location of the events within the network and other analyses.

In order to obtain a reasonable homogeneous model we calculate an average velocity defined to be the distance between focus and station divided by the travel time based on the standard layered model derived by the Kurayoshi and Hanabusa explosions. Such a velocity as a function of epicentral distance and focal depth is described in Fig. 2.

4. Hypocenter location and travel time anomalies

The hypocentral distribution in and around Tottori is shown in Fig. 3. The method of hypocenter location and the data used are presented in the appendices. Calculations were carried out for the P velocity 5.8 and 6.0 km/s of the assumed homogeneous medium. For the sake of simplicity any correction concering the stations, for instance, height corrections, is not taken into account. In the figure the solution with the shallowest focus is plotted.

Very shallow events are found in the Hamasaka, Tottori, Misasa and Chizu regions. Earthquakes with a focal depth of more than 15 km have been occurring in the Sayo region. In the vicinity of the Yamasaki fault the focal depths range from 10 to 15 km. Most of the focal depths in the figure are restricted to 5–15 km.

Another aim of the hypocenter location is to get valuable information as to the crustal structure. When a homogeneous medium is assumed, then the four source parameters (three coordinates and origin time) and the constant P velocity of the medium are altogether obtained in terms of P arrival times at certain five stations. Practically, the determination of the source parameters by each network of four stations are carried out taking the velocity as a parameter as described in Appendix 1.

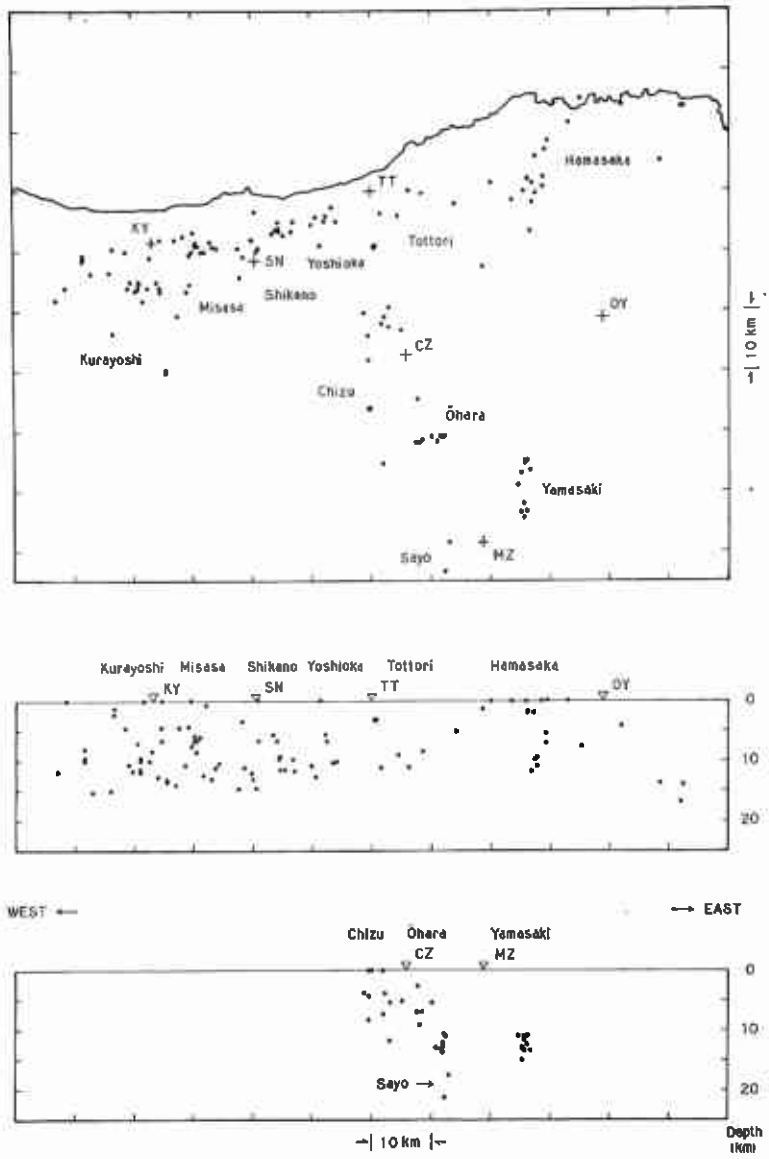

Fig. 3. Spatial distribution of hypocenters listed in Table 6. The coordinates of the events plotted are those of the shallowest focus of the two sets of solutions which are obtained for the crustal P velocity 5.8 and 6.0 km/s respectively.

This idea was applied to the events located within the network of *TT*, *CZ*, *KY*, *OY* and *MZ*. In the first place the hypocenter determination was carried out in the case of *TT*, *CZ*, *KY* and *OY* stations. And then, instead of *OY*, *MZ* was used as a station of another quadrant network. The results reveal that in some cases the two solutions of hypocenter differ greatly from each other for any given velocity. This fact indicates the existence of lateral heterogeneity within the above networks.

But this is not the case for the events in the Tottori and Yoshioka regions.

The summary of the above analyses is given in Table 2 and Fig. 4. *O–C* times (the differences between observed travel times and culculated ones) at *MZ* station are listed in Table 2. Each focus is determined by the use of *P* times of *TT*, *CZ*, *KY* and *OY* stations and plotted in Fig. 4. Solid circles show the events from which *P* delays are observed at *MZ*. The focal depths of all the events range from 3 to 15 km.

Generally the *O–C* times are smaller for the velocity 6.0 km/s than 5.8 km/s.

Table 2. Differences between the obsevational and calculated travel times at *MZ* station

No.	Date			Origin Time		Region	Focal Depth	O–C	Vo
	Y	M	D	H	M		(km)	(sec)	(km/s)
1	1973	9	18	20	44	Tottori	6.9	−0.06	5.8
							3.5	0.03	6.0
2		9	23	09	34		7.2	0.01	5.8
							4.0	0.08	6.0
3				12	24		6.6	−0.05	5.8
							3.1	0.04	6.0
4		11	7	19	51		9.0	−0.11	5.8
							5.3	0.01	6.0
5	1974	1	4	21	23		11.0	−0.11	5.8
							8.5	0.00	6.0
6		2	17	04	16		10.6	−0.11	5.8
							8.9	0.01	6.0
7	1973	7	27	06	37	Yoshioka	12.1	−0.12	5.8
							10.4	0.02	6.0
8	1975	8	27	11	54		10.6	−0.13	5.8
							8.1	−0.01	6.0
9	1973	11	11	06	45	Shikano	13.3	−0.04	5.8
							9.7	0.03	6.0
10	1974	2	7	04	29		15.3	−0.07	5.8
							11.5	−0.01	6.0
11				04	30		15.4	−0.07	5.8
							11.5	−0.01	6.0
12	1975	11	14	16	36		11.9	0.06	5.8
							6.8	0.13	6.0
13	1973	4	12	17	33		19.4	0.21	5.8
							14.9	0.22	6.0
14		4	17	15	49		17.8	0.45	5.8
							11.1	0.41	6.0
15	1974	7	22	07	32		17.3	0.10	5.8
							12.8	0.13	6.0
16	1973	4	23	10	30	Misasa	23.3	0.53	5.8
							14.0	0.42	6.0
17		4	24	15	15		20.9	0.29	5.8
							10.9	0.18	6.0
18				15	17		18.0	0.25	5.8
							6.6	0.12	6.0
19	1974	7	17	05	12		17.9	0.55	5.8
							6.8	0.45	6.0

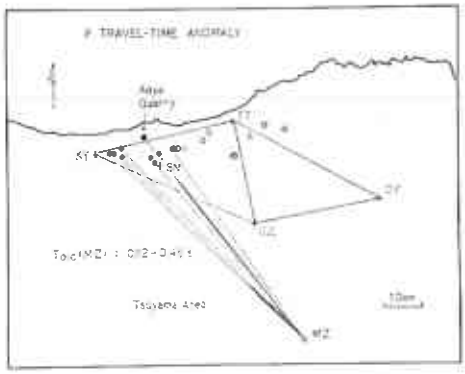

Fig. 4. Distribution of epicenters listed in Table 2. Solid circles indicate the events for which the anomaly in travel times was observed at *MZ* station and open circles mean the events which indicated no anomaly.

Therefore it is concluded that the average velocity of the crust beneath the network concerned is about 6.0 km/s and not less than 5.8 km/s. It is found to be consistent with the velocities given in Fig. 2 taking account of the epicentral distances (10–60 km) and focal depths.

The locations of events which show travel time anomalies at *MZ* are restricted to the western part of the Shikano region and the Misasa region. Because the delay times of 0.12–0.45 sec are far beyond the limit of reading error, they should be ascribed to the lower velocity structures in some regions. It must be noted that the epicentral distances are larger for *MZ* than *OY* and the low apparent velocity is not due to the shallow seismic-wave path. The data from quarry blasts fired at Aoya (See Fig. 1) also indicate the *P* delay to be about 0.2 sec at *MZ* station, as will be pointed out in the next section.

The anomalous region should not be included in the area in and just outside the Shikano and Misasa regions, because no travel time delay is found at *KY* in the analysis of events located in the Yamasaki region. The calculated travel times by the use of the foci determined by the *P* times of *CZ*, *MZ*, *OY* and *IZ* agree well with the observed ones at *KY* as well as *TT* for the crustal velocity 6.0 km/s. Eventually the low velocity zone is estimated to be somewhere around Tsuyama (Fig. 4).

5. Aoya quarry blasts

In addition to natural earthquakes quarry explosions fired at Aoya are analysed to obtain more detailed structure of the upper crust. The location of the shot point is:

35°28′48.5″N
133°58′29.5″E,

and the height is 50–100 m above sea level. Strictly speaking the locations of the shot points are different from one another by 100 m or so. In the present study

the above differences are neglected.

From April to December in 1975, seven shots were observed at *TT* station and some of them were detected at more distant stations. An example of seismograms of the blasts recorded at *TT* is presented in Fig. 5. The arrival times are plotted as a function of distance in Fig. 6, where *SN* station is taken as a standard of *P* times. Data of *KY* is largely scattered in comparison with other stations owing to the high level of ground noise since the blasts were always carried out toward evening when the level of such noise as traffic vibrations is very high.

Along the profile passing through *TT*, *CZ* and *OY* stations the apparent velocity is 6.05 km/s, which is consistent with the results of the Kurayoshi and Hanabusa explosions. On the other hand at *MZ*, *IZ* and *HM* the travel times delay is about 0.2 sec in comparison to the travel times along the above profile. It is remarkable that the travel path to *MZ* station crosses the anomalous area revealed by the micro-

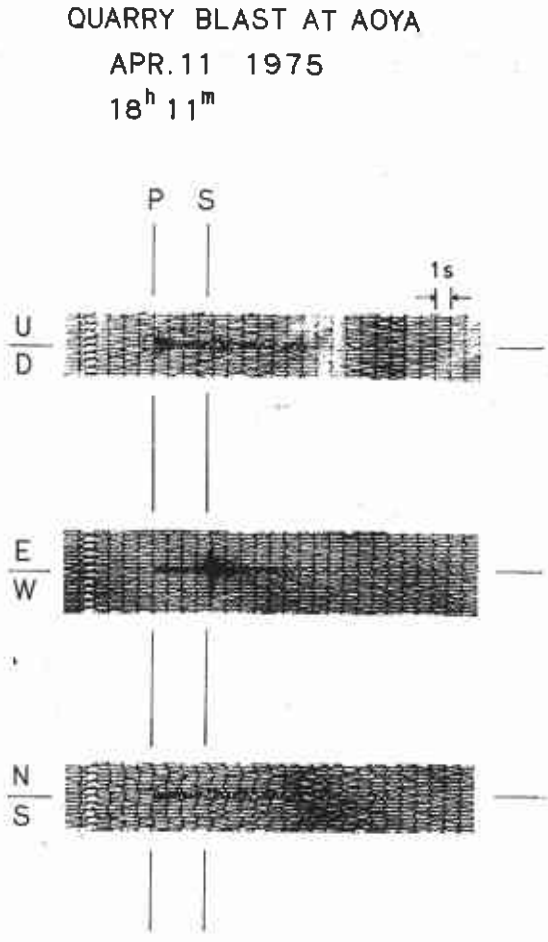

Fig. 5. An example of the seismograms of the Aoya quarry blasts recorded at *TT*.

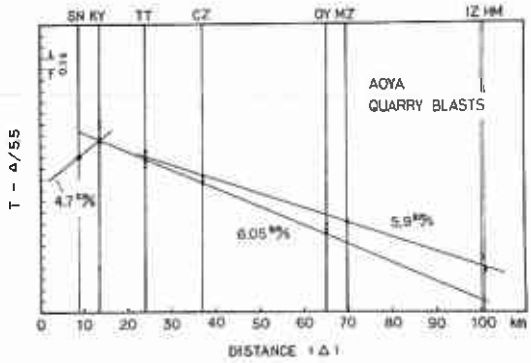

Fig. 6. Arrival times of the Aoya quarry blasts. *SN* station is taken as a standard.

earthquake study presented in Section 4.

The apparent velocity for the uppermost layer is 4.7 km/s as seen from Fig. 6. Mino et al.[17] reported the apparent velocity derived by a tripartite observation in the Yoshioka region as 4.75 km/s. According to these results the velocity of the superficial layer in the Yoshioka, Shikano and Misasa regions is estimated to be 4.5–5.0 km/s. Its value is lower than that given in the crustal model of the Kurayoshi and Hanabusa explosions[16].

6. V_p/V_s

S velocity structures will be discussed in terms of the velocity ratio of *P* to *S*(V_p/V_s) inferred from the *P* times and *S*–*P* times. When a homogeneous half space is assumed the following linear relation is established:

$$t_p=\alpha t_{s-p}+\beta \qquad (1)$$

where t_p and t_{s-p} are *P* arrival time and *S*–*P* time respectively and α and β are constants. Then V_p to V_s ratio is given as follows:

$$V_p/V_s=\frac{\alpha+1}{\alpha} \qquad (2)$$

The constant β in (1) is equivalent to the origin time. The V_p/V_s ratio determined by the use of formula (1) is considered to be that of a first approximation when applied to the field observations.

The method of least squares is applied to fitting *P* and *S*–*P* times of a micro-earthquakes to (1). The data with *S*–*P* times less than 10 sec and the accuracy of readings 0.1 sec for *P* and 0.2 sec for *S* were used. The list of the V_p/V_s value of each event is presented in Appendix 2. The regional mean values of V_p/V_s together with their standard deviations were calculated and listed in Table 3. The distribution of the regional mean values are shown in Fig. 7.

The V_p/V_s values derived by the present study are slightly lower than those deter-

Table 3. Regional variation of V_p/V_s.
PS denotes $S-P$ time in seconds observed at *TT*

Region	V_p/V_s			Focal Depth (km)				
	Number of Data	Mean	Standard Deviation	for V=5.8 km/s		for V=6.0 km/s		Number of Data
				Mean	Standard Deviation	Mean	Standard Deviation	
Hamasaka 5.4≤PS≤6.3	4	1.69	0.02	17.1	7.2	12.2	5.5	4
Hamasaka 2.6≤PS≤4.5	18	1.70	0.02	11.1	4.4	4.3	4.6	18
Tottori 1.4≤PS≤2.0	8	1.69	0.03	7.9	3.8	6.6	4.0	8
Yoshioka 1.4≤PS≤2.1	10	1.67	0.05	10.1	2.2	9.8	3.8	7
Shikano 2.2≤PS≤2.5	8	1.66	0.08	10.0	4.3	8.2	4.0	8
Shikano 2.7≤PS≤3.2	9	1.70	0.05	13.1	6.1	10.5	5.4	7
Misasa 3.3≤PS≤4.0	17	1.68	0.05	11.8	6.5	9.4	3.0	12
Kurayoshi 4.3≤PS≤5.0	20	1.68	0.04	10.4	4.7	7.3	5.2	19
Kurayoshi 5.1≤PS≤6.6	10	1.67	0.05	10.1	4.8	9.0	6.0	10
Chizu 2.5≤PS≤3.5	8	1.70	0.03	7.9	2.1	6.6	3.0	8
Chizu 4.4≤PS≤5.0	7	1.66	0.03	4.4	1.2	0.4	1.0	7
Ohara 5.3≤PS≤5.4	11	1.69	0.03	13.3	2.3	10.6	2.9	11
Yamasaki 6.3≤PS≤7.1	10	1.71	0.03	13.8	2.6	12.9	2.0	11

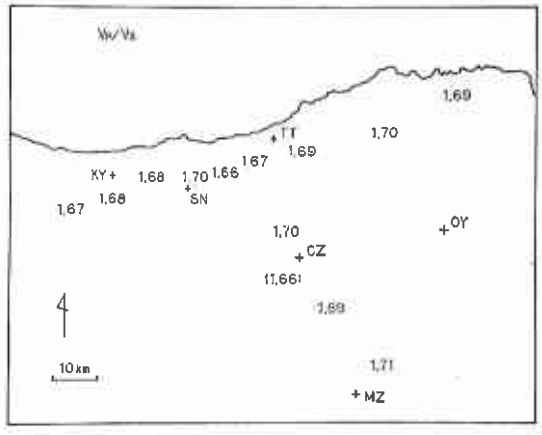

Fig. 7. Distribution of V_p/V_s. The parenthesized value is questionable.

mined by Hashizume in 1970[4] except for the Yamasaki and Sayo regions. Particularly the western regions show low V_p/V_s structures.

Focal depths in various regions are summarized in Table 3 in order to examine the effect of the depth of focus on the apparent V_p/V_s. When the Yamasaki and Sayo regions are compared with other regions where shallow events are predominant it seems to suggest that for deep events V_p/V_s values are high. Hashizume[4] derived the depth distribution of V_p/V_s in the crust. According to him the V_p/V_s values are nearly constant as 1.70–1.71 above the depth of about 13 km and below that increase with the increase of depth at a considerable rate. It is difficult to reveal the detail of the depth dependence of V_p/V_s because the spacing of the stations available is not tight enough to cover the wide range of epicentral distances.

In the Chizu region (4.4 sec$\leq S$–P time at $TT\leq$5.0 sec) very low V_p/V_s values were obtained. But there is the possibility that the S waves on the vertical component seismograms recorded at CZ might have been confused with other phases. These earthquakes almost belong to the aftershocks of the earthquake of 1972. Because of shallow foci the waveforms at the nearby station (CZ) are very complicated and the most prominent phase of each event was primarily interpreted to be the direct S wave. If the interpretation is correct the V_p/V_s value in the uppermost part of the crust should be very low. In this paper we cannot present any conclusion about that.

Standard deviation of V_p/V_s values in the Shikano region (2.2 sec$\leq S$–P time at $TT\leq$3.5 sec) is considerably larger than other regions though the quality of data is not so bad. It might indicate some complicated crustal structure in the region.

From a statistical point of view the regional variation of V_p/V_s is not so significant. For instance when t-statistics for two means is applied to the V_p/V_s values of the Yoshioka and the Shikano (2.7 sec$\leq S$–P time at $TT\leq$3.2 sec) regions, the null hypothesis that the two means are equivalent cannot be rejected with a level of significance below 10%.

Nevertheless the results may be useful for understanding the V_p/V_s structure in each region. The P and S–P time data are plotted altogether in respective regions taking the data of TT as standards in Fig. 8. In the diagram we can determine α given in (1), and Eq. (2) provides V_p/V_s values. This is another method for deriving an average value of V_p/V_s in a region.

7. Angles of incidence of P waves at TT

Angles of incidence are calculated using the amplitudes of vertical and two horizontal components of initial motions. These amplitudes are measured on the seismograms as illustrated in Fig. 9. Table 4 is the list of the mean values of the angles of incidence for respective regions where the events originated. In a similar manner we can obtain approximate values of the angles by the use of maximum amplitudes of the three respective components of the P wave trains instead of initial motions. The results are also given in Table 4.

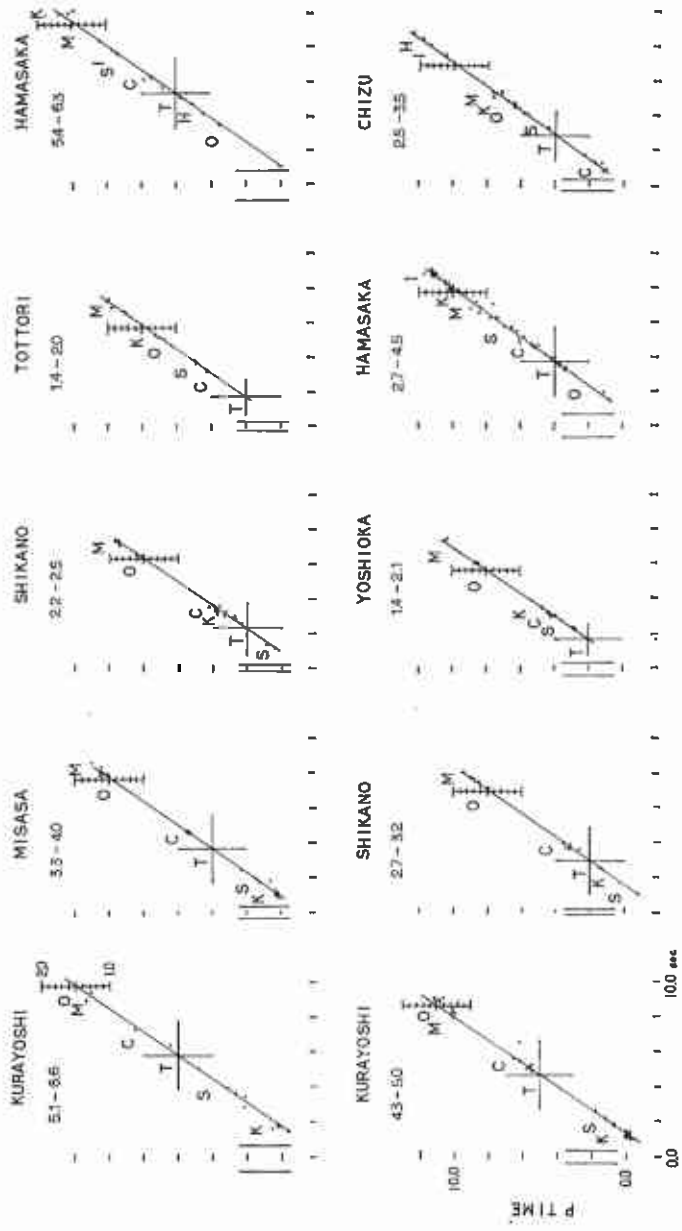

Fig. 8. V_p/V_s determination in each region. *TT* station is taken as a standard. The range of $S-P$ time at *TT* in each region is inserted in the figure.

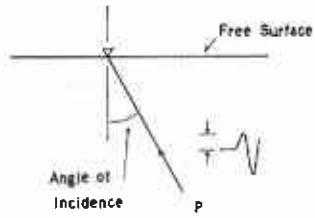

Fig. 9. Illustration of an angle of incidence.

Table 4. Angles of incidence at *TT* derived by the amplitudes of the initial motion and the maximum amplitudes of the *P* waves. Mean values for the events of respective regions are listed together with standard deviations

Region	For Initial Motion		For Maximum Amplitude of *P*	
	Number of Data	Angle of Incidence at *TT* (°)	Number of Data	Angle of Incidence at *TT* (°)
Yamasaki, Sayo	11	39.3±10.2		
Ohara	2	28.6±10.7	2	21.0±1.2
Chizu	4	35.9± 4.5	1	33.2
Hamasaka	5	37.7± 4.6	2	34.3±3.6
Tottori, Yoshioka	1	29.5	6	30.7±7.9
Shikano	2	32.4± 4.0	9	33.2±8.2
Misasa, Kurayoshi	12	28.9±12.8	8	35.3±8.8

The incident angles above obtained are in the range from 29° to 40°. When we take the *P* velocity of the deepest point of the ray as 6.05 km/s, assuming that the angles of emergence measured from the vertical are nearly 90°, then the *P* velocity of the soft layer just blow the Tottori station can be estimated to be 2.9–3.9 km/s.

8. *SxS* phases recorded at TT

On the seismograms of local microearthquakes with *S*–*P* times 0.7–1.5 sec recorded at *TT* station we often find remarkable phases which follow the direct *S* waves by about 4–8 seconds. They are not recognized on vertical component seismograms. And the frequencies of the oscillations are as high as direct *P* and *S* waves. Probably they are not surface waves, which would be rich in low frequency oscillations owing to dispersion and attenuation. Therefore we can regard the phases as either *SH* waves coming from just below the observation point or *P* waves travelling along the ground surface. Except for a few cases the microearthquakes with close distances less than about 15 km from *TT* seem to have such phases although the recognition is difficult when the events are either too small or too large.

Similar phases were found for the events originating in the Wakayama region, Southern Kinki, Japan, by Mizoue[16]. He interpreted these phases as reflected *S*

waves (SxS) at the Conrad discontinuity in the crust and derived the depth of the discontinuity by travel time-distance relations. The reflected P waves (PxP) were also recognized for rather distant events with $S-P$ times of 4–8 seconds.

It is expected that also in the case of Tottori the phases can be interpreted as SxS waves reflected at a certain discontinuity. The travel time difference between SxS and direct S is as follows:

$$T_{sxs}-T_s=\frac{\sqrt{(2H-h)^2+\Delta^2}-\sqrt{h^2+\Delta^2}}{V_s}, \tag{3}$$

or

$$=\frac{\sqrt{(2H-h)^2+k^2t^2_{s-p}}-h^2-kt_{s-p}}{V_s}, \tag{4}$$

where

$$k=\frac{V_p}{V_p/V_s-1}, \tag{5}$$

$$t_{s-p}\geq\frac{h}{k}, \tag{6}$$

and H, h, Δ, V_p, V_s and t_{s-p} denote depth of the discontinuity, focal depth, epicentral distance, P velocity, S velocity and S–P time, respectively as illustrated in Fig. 10. In the above equations it is implicitly assumed that the boundaries are horizontal and the medium between them is uniform.

Table 5a, b is the list of events with fairly recognized SxS waves. Examples of seismograms are presented in Fig. 13a, b. The reflected waves provide a powerful method of investigating the structure of the crust as pointed out by Kamitsuki[19], who analysed S_MS waves (reflected waves at the Mohorovičić discontinuity). We want to determine the depth of the discontinuity, which would be situated at the depth of about 16 km. The earthquake foci should be within a distance of 15 km or so from the station judging from the S–P times. If we take h as 16 km in the graph given in Fig. 2 the average P velocity of the upper crust is about 5.93 km/s for epicentral distances 0–15 km. The V_p/V_s value in the Tottori region is about 1.69 as shown in Fig. 7. We assume that the P and S velocities are 5.9 and 3.5 km/s respectively. In this case k (Ōmori coefficient) is obtained as 8.55 from (5).

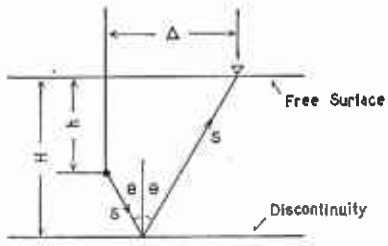

Fig. 10. Ray path for a SxS wave.

Table 5a. List of the events accompanied with *SxS* phases for $S-P$ times at *TT* less than or equal to 1.0 sec.

No.	Date			Origin Time		Mag.	*PS* Time at *TT*	*Tsxs-Ts*
	Y	M	D	h	m		(sec)	(sec)
1	1971	9	18	03	32	0.3	1.0	4.3
2	1973	4	19	03	52	0.4	1.0	5.4
3		5	27	20	20	0.4	0.8	7.6
4		8	19	19	37	0.4	0.8	5.6
5		11	3	27	10	0.4	0.8	5.9
6		11	4	04	07	0.4	0.8	5.9
7		11	28	04	34	1.3	0.7	5.5
8	1974	7	20	18	50	0.4	0.9	5.2
9		10	3	07	30	1.3	0.9	5.2
10		12	18	03	16	0.8	1.0	5.2
11	1975	2	2	05	59	0.1	0.7	6.5

Table 5b. List of the events accompanied with *SxS* phases for $S-P$ times at *TT* more than 1.0 sec.

No.	Date			Origin Time		Mag.	*PS* Time at *TT*	*Tsxs-Ts*
	Y	M	D	h	m		(sec)	(sec)
1	1972	2	14	01	14	0.4	1.1	4.7
2		3	7	21	01	0.4	1.2	4.8
3		6	26	12	26	0.4	1.4	4.4
4		10	11	05	28	1.3	1.4	4.5
5		10	25	17	56	0.4	1.1	5.2
6		12	18	04	36	0.4	1.1	5.0
7	1973	1	13	10	48	0.9	1.2	4.5
8		6	10	08	08	0.9	1.1	7.0
9		7	27	06	37	1.6	1.4	5.1
10		9	5	03	35	0.7	1.4	5.0
11		9	7	06	00	0.4	1.3	5.0
12		10	8	23	07	0.7	1.1	4.6
13		11	16	19	42	0.8	1.4	4.8
14		12	2	06	22	0.4	1.1	4.9
15	1974	1	4	21	23	1.3	1.5	4.0
16		1	16	04	21	0.3	1.4	4.0
17		3	30	17	51	0.4	1.3	4.2
18		5	4	13	01	1.3	1.4	5.6
19		8	2	04	43	0.8	1.3	6.5
20		8	24	05	11	0.7	1.3	7.1
21		8	24	06	48	0.9	1.2	6.7
22		10	30	02	29	1.6	1.5	3.5
23		10	30	06	12	0.9	1.4	4.2
24	1975	4	6	07	32	0.9	1.4	4.6
25		4	8	00	22	1.8	1.5	4.0
26		4	18	18	20	0.4	1.1	5.0

If the locations of the events are known we can derive the depth of the discontinuity by Eq. (3). However, only a few of them can be located as presented in Table 6. Most of the events are so small in magnitude that they cannot be observed at distant stations. Located events will be discussed later and we take here another approach.

Since *S–P* times are known, then Eq. (4) is useful. From (6) the travel time difference should satisfy the following relation:

$$T_{sxs}-T_s \geq \frac{2H-h-kt_{s-p}}{V_s} \tag{7}$$

The right hand side is a linear function of H (depth of the discontinuity) and t_{s-p} (*S–P* time). Applying (7) to the travel time differences and *S–P* times listed in Table 5a, b, it is concluded that the depth H is less than 16 km. Another test is given as follows:

$$T_{sxs}-T_s \leq \frac{\sqrt{4H^2+k^2t^2_{s-p}}-kt_{s-p}}{V_s} \tag{8}$$

The above relation is established by reason that *Tsxs-Ts* decreases monotonously with focal depth h and h should not be negative. This test indicates that the interface is deeper than about 16 km. Then, the discontinuity beneath the Tottori region should be situated at the depth of 16 km which corresponds to that of the Conrad discontinuity derived by the Kurayoshi and Hanabusa explosions (See Fig. 2).

Based on the above result the calculated curves of Eq. (4) together with the data used are described in Fig. 11. It shows that there are two groups of events; the events of one group are very shallow and those of the other group are confined to

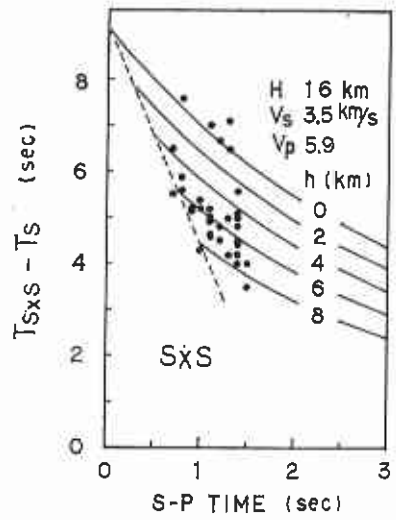

Fig. 11. Observed and calculated $SxS-S$ times versus $S-P$ times. The data are listed in Table 5a, b. The dotted line indicates the boundary given by Eq. 7.

the depth range from 4 to 8 km. Between the two groups there is a considerable gap.

The amplitude ratio of *SxS* to *S* of each event is about 0.1, which can be explained by the reflectivity calculated by the theory of elasticity if we assume both the velocity and density ratios across the discontinuity as 1.1 or so taking account of small reflection angles.

The very shallow events of the first group do not seem to be explosions. Some of them show dilatation in initial motions as the shock of August 24, 1974 of which seismogram is presented in Fig. 13a. Therefore, we can safely say that in the Tottori region very shallow microearthquakes with the focal depth 0–2 km are occurring.

It is also remarkable that the data with *S–P* times 1.6 sec or more are absent. This is partially because the frequency of *S–P* times of 1.6–2.0 sec is less than half of those of 1.0–1.5 sec. Moreover there seems to be the case that the travel time differences (*SxS–S* time) is small enough to be unable to distinguish the *SxS* phase from the direct *S* phase for a deep focus. When travel time difference is less than about 3 sec it is difficult to recognize the *SxS* phase. The absence of data probably means that the depths of the events with *S–P* times 1.6 sec or more are larger than about 8 km and *SxS–S* times are less than the limit (about 3 sec).

As far as the Tottori area the detected *SxS* waves are entirely of the *SH* type. No *SV* type has been observed. This is probably because the microearthquakes of dip-slip faulting are quite small in number, and the majority of the shocks are of strike slip type. On the contrary Sanford et al.[20),21)] found *SV* waves reflected at the Conrad discontinuity in Socorro, New Mexico, where dip-slip faulting seems to be frequently occurring.

By the use of the calculated *SxS* times presented in Fig. 12 we can discuss focal depths. The shock of July 27, 1973 is located by using *P* arrival times of four stations (*TT*, *CZ*, *OY*, *MZ*) as given in Table 6. The epicentral distance and focal depth for *P* velocity 6.0 km/s are 7.0 km and 10.4 km respectively. From Fig. 12 the *SxS–S* time is obtained as 3.2 sec. However the *SxS–S* time given in Table 5b

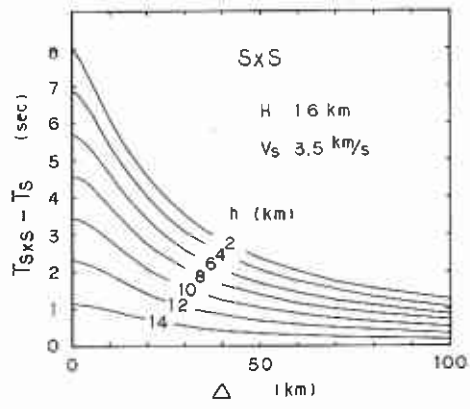

Fig. 12. Calculated curves of *Tsxs-Ts* as a function of epicentral distance.

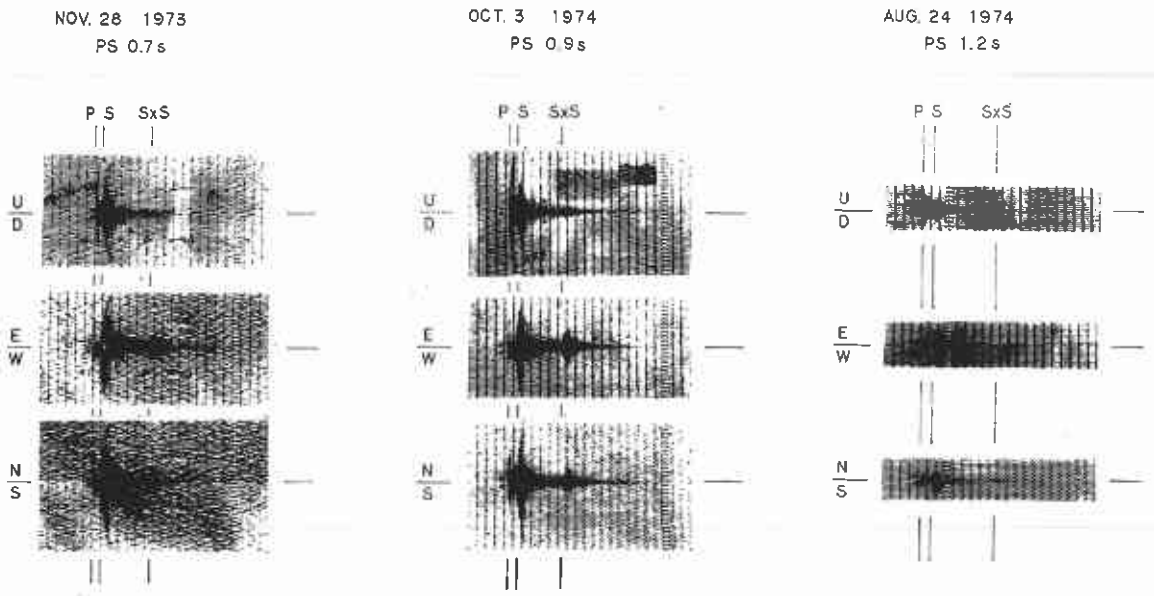

Fig. 13a. Examples of the seismograms accompanied with *SxS* phases recorded at *TT*. PS means $S-P$ time in seconds.

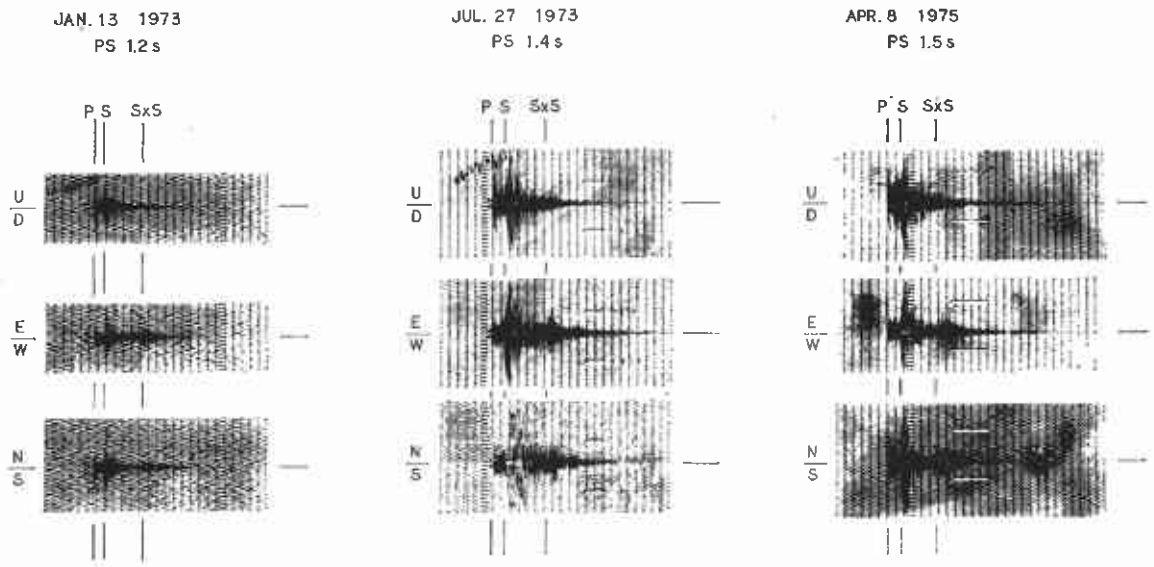

Fig. 13b. Examples of the seismograms accompanied with *SxS* phases recorded at *TT*.

is different from the calculated one. This means either the *SxS–S* time should be shortened in reading the seismogram, or the true focal depth is less than that calculated.

9. *SxP* phases recorded at TT

S waves of microearthquakes treated in the present study have predominant *SH* components excepting those of the earthquake swarm of April, 1973, at the Misasa region. Some events of the swarm are located and listed in Table 6. An example of seismograms is shown in Fig. 16. Notice that the radial component (*E–W*) of the *S* wave is predominant. Epicentral distances of them are around 30 km and focal depths are confined to the range from 4 to 14 km. The scattered values of the depth must be due to inevitable reading errors. Then the *SxS–S* time should be within the range from 0.5–3.0 sec.

A late arrival which follows the direct *S* by 0.6 sec is found on the seismograms of the swarm (see Fig. 16). This is not the *SxS* phase. Because the reflected wave should be incident at a smaller angle of incidence than the direct *S* wave. The phase is prominent in the vertical component although the direct *S* wave is almost horizontally polarized.

The above-mentioned phase can be explained as the *SxP* wave which is illustrated in Fig. 14. The calculated *SxP–S* times shown in Fig. 15 indicate that the focal depth is about 3–4 km. In this discussion we implicitly assume that the structure is the same as that used in the last section. At that depth the *SxS–S* time should

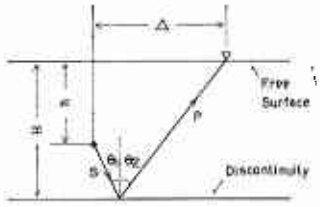

Fig. 14. Ray path of a *SxP* wave.

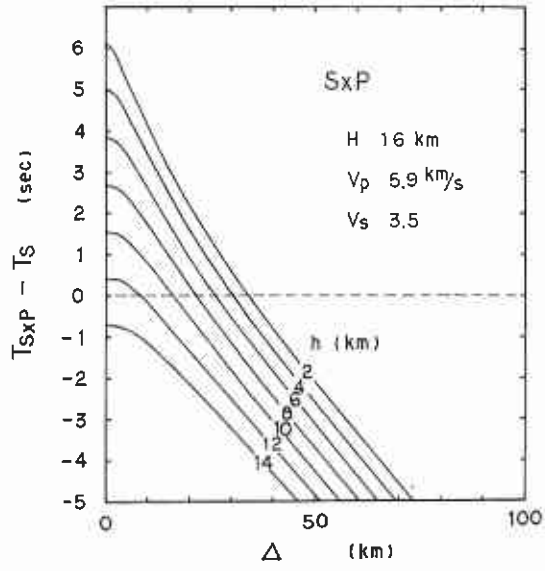

Fig. 15. Calculated curves of *Tsxp-Ts* as a function of epicentral distance.

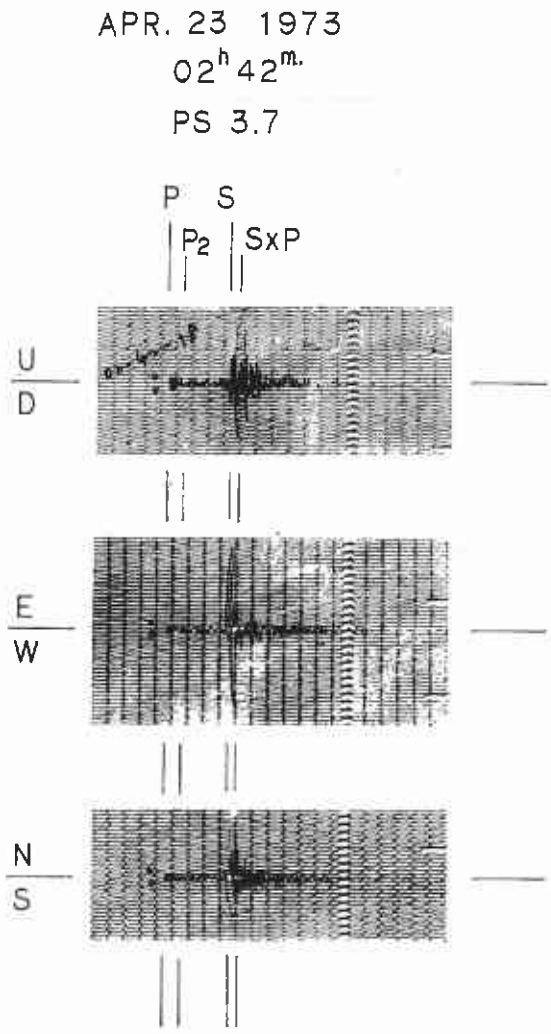

Fig. 16. An example of the seismograms of the swarm of April, 1973, Misasa, recorded at *TT*.

be 3.0–3.5 sec (See Fig. 12). But this phase is not clearly recognized on the seismogram.

10. *SP* phases recorded at *TT*

The wave which is emitted at the origin as a *SV* wave and is converted to a *P* wave at the free surface is defined as a *SP* wave as illustrated in Fig. 17. This type of phase was found in two cases. The one is the shock of September 30, 1974 and the other is the swarm of October, 1971. These events occured in the Hamasaka region and are characterized by very shallow hypocenters. Their seismograms are

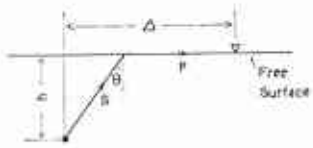

Fig. 17. Ray path of a *SP* wave.

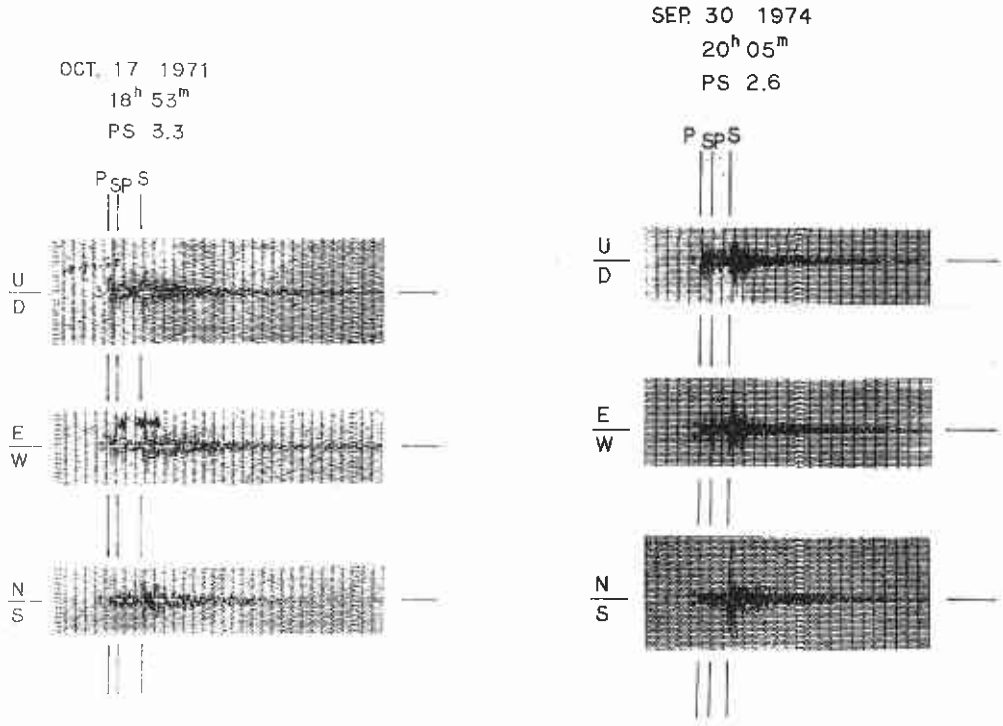

Fig. 18. Seismograms accompanied with *SP* phases recorded at *TT*. The events originated in the Hamasaka region.

shown in Fig. 18. The direction of approach is nearly the east and the wave is prominent in the horizontal E–W component.

The *SP–P* time is calculated by using the same crustal model as used in Section 8 (Fig. 19). The both events have the *SP–P* time of 1.0 sec and their epicentral distances are in the range from 20 to 30 km. Then, the focal depth derived by the *SP* phase is about 5 km. This depth is somewhat larger than the values obtained by the hypocenter location.

Fig. 20 is the seismogram of the event which occurred at almost the same epicentral region as the shocks of October, 1971. But the *SP* phase is not recognized on this seismogram although the direct *SV* wave is not small in amplitude. The shock of May, 1975 shown in Fig. 20 originated at the depth of 9.5–14.3 km according to Table 6. Therefore it is concluded that for a deep focus as this event the *SP* phase

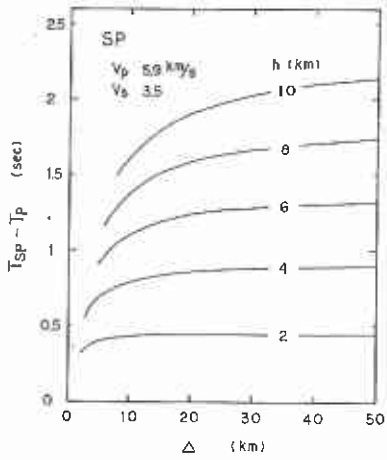

Fig. 19. Calculated curves of *Tsp-Tp* as a function of epicentral distance.

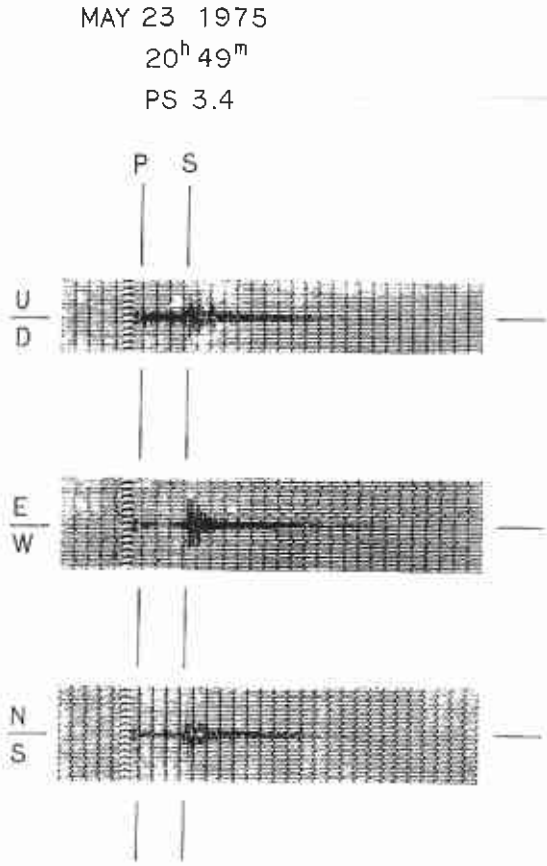

Fig. 20. Seismogram of the shock which originated in the Hamasaka region. Compare its waveform with that of the shock of Octover, 1971 shown in Fig. 18.

cannot be recognized. In the case of shallow focus and close epicentral distance the *SP* wave becomes a remarkable marked phase as pointed out theoretically by Kawasaki et al.[22].

11. Discussions on waveforms of various regions

The waves discussed in Section 8 and 9 are those of microearthquakes which originated in the Tottori and Misasa regions respectively. In this section we will present some representative waveforms from other regions and discuss some prominent phases in connection with the crustal structure and focal depths.

Ohara region:

In the Ohara region microearthquake swarms were found twice in March, 1974

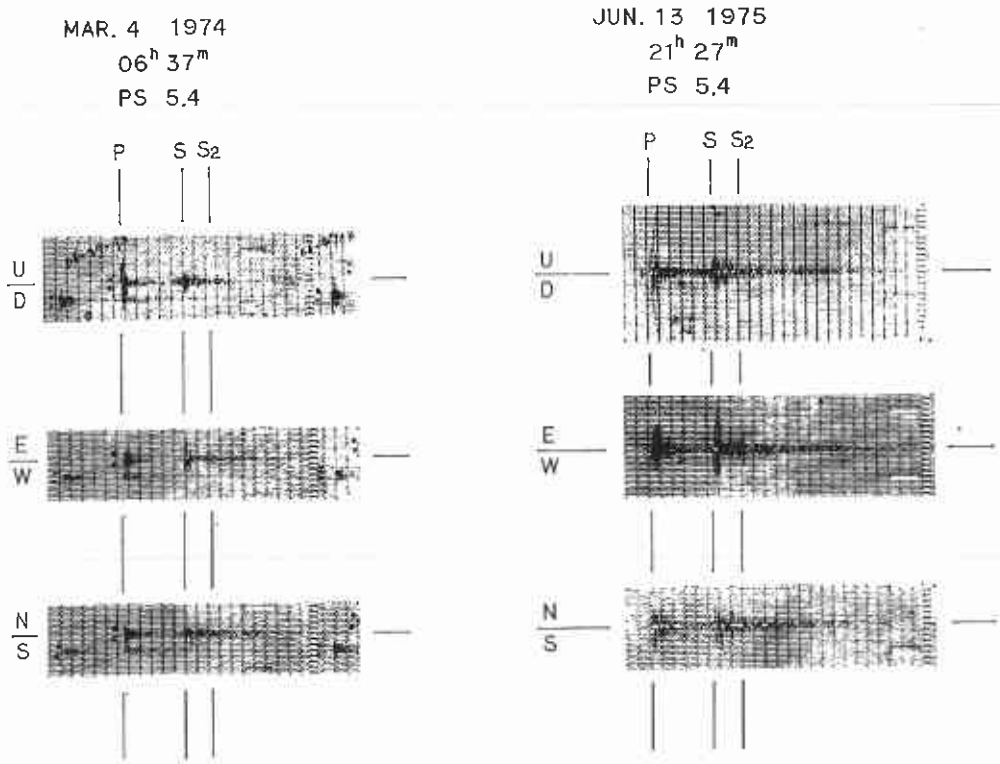

Fig. 21. Seismograms of the swarms which originated in the Ohara region in March, 1974 and June, 1975.

and June, 1975. Examples of their seismograms are presented in Fig. 21. The waveforms of the two groups are quite similar to each other. The S waves are predominant in SH motions as seen from the seismograms recorded at TT which is located nearly to the north of the source region.

The phase S_2 indicated in the figure is also a SH wave and has an impulsive waveform like the direct S wave. The onset of S_2 is clear and its sense is reverse to that of the direct S. The above nature would indicate that S_2 is a reflected wave (SxS) at the rigid boundary which is probably the Conrad discontinuity.

Let us derive the depth of the boundary by use of Eq. (3). The values of the parameters are as follows: V_s=3.5 km/s, Δ=42.9 km, h=12.5 km and $Tsxs$-Ts=2.4 sec. The above epicentral distance and focal depth are the average values obtained for the events by the use of the hypocentral coordinates presented in Table 6 for the P velocity 6.0 km/s. The SxS–S time is measured on the seismograms given in Fig. 21. Then the depth is estimated to be about 22 km. This result seems to suggest that the Conrad discontinuity below the Tottori area dips southward with a depth of 16 km in the Tottori region and 22 km in the Chizu and Ohara region.

Hamasaka region:

Fig. 22 shows another example of shallow events located in the Hamasaka region

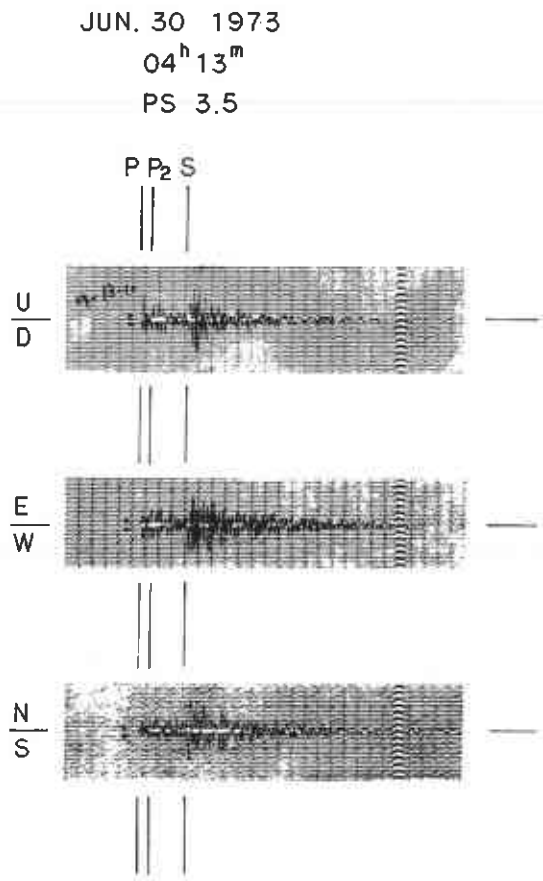

Fig. 22. Seismogram of the shallow shock which originated in the Hamasaka region.

to the east of Tottori. The phase marked as P_2 is probably something like a *SP* wave. The oscillatory nature and somewhat large vertical amplitude would be due to the superficial layer through which the wave was propagated. The epicentral distance is about 30 km. Then from Fig. 19 and taking *Tsp-Tp* as 0.6 sec we obtain the focal depth as 3 km. This depth is consistent with that determined by *P* times (Table 6).

Similar waves are found in the case of the swarm of 1973 at Misasa which was treated in Section 9 (Fig. 16). The *SP–S* time is about 0.9 sec. Therefore, from Fig. 19 the depth of the events should be in the range from 4 to 5 km. This depth is consistent with the result from the *SxP* phase.

The velocity of *P* in the superficial layer is estimated to be 3.0–5.0 km/s from the discussions in Section 5 and 7. The waves of the *SP* type would be trapped in this layer.

Shikano region:

Two examples of the waveforms which originated in the Shikano region are presented in Fig. 23. The shock of April, 1973 is a example of deep events with focal depth 10–15 km. On its seismogram no prominent phase can be recognized. On the other hand the shock of November, 1973 has a peculiar phase which follows direct *P* phase by 0.9 sec. Such a phase is not seen in other earthquakes which occurred in this region. It can be considered that the above phase is something like an *SP* wave. If so the focus should be very shallow with its depth about 5 km. However the focal depth obtained by *P* times is 9.7 km for the *P* velocity 6.0 km/s. For the above difference no explanation can be given in the present study.

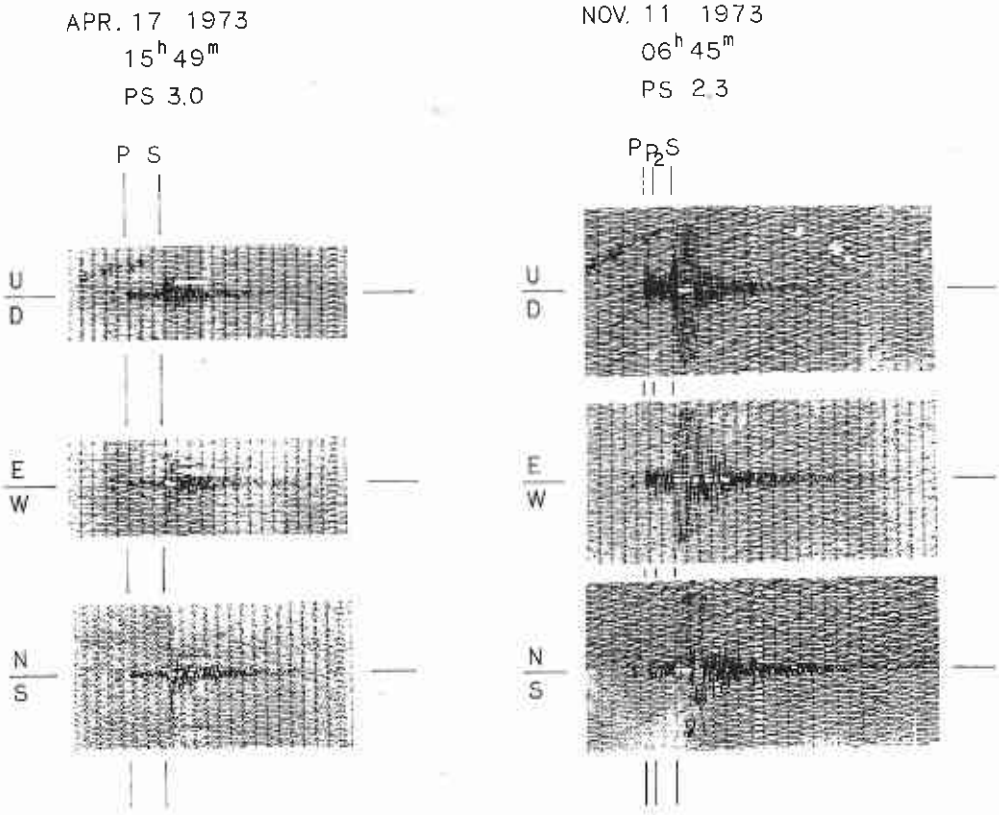

Fig. 23. Seismograms of the shocks which originated in the Shikano region.

Chizu region:

Fig. 24 shows the shock of October 18, 1972 (M3.3) which occurred in the vicinity of *CZ* station and 36 km to the south of *TT* at the depth of 0–5 km. The initial motion reasonably indicates that the *P* wave is incident from the south. To the contrary, as seen from the figure the wave marked as P_2 has considerable transversal

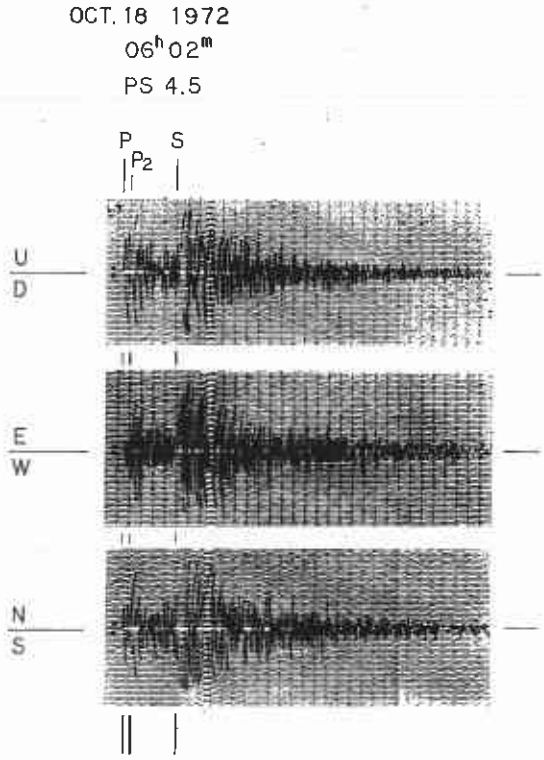

Fig. 24. Seismogram of the shock which originated in the Chizu region.

motions.

In the laterally homogeneous medium the transversal wave should be an *SH* type which cannot be transformed to other type of waves, i.e., *P* and *SV* waves. But we cannot interpret the P_2 phase as an *SH* wave. For it should arrive after the direct *S* wave.

The nature of the above P_2 phase may be explained by the lateral heterogeneity of the uppermost part of the crust.

12. Conclusion

The results of the present study on the waveforms and travel times of microearthquakes and quarry blasts which originated in and around the Tottori area are as follows: (1) Angles of incidence of *P* at *TT* derived by the initial motions are about 29°–40° for various events. And it is suggested that the velocity of the uppermost layer of the crust just below Tottori is about 2.9–3.9 km/s for *P*. Data from the quarry blasts at Aoya indicate the *P* velocity of the superficial layer as 4.7 km/s. (2) The layer of the *P* velocity 6.05 km/s was confirmed along the profile which passes through *TT*, *CZ* and *OY* by using the travel times of the Aoya quarry explosions. *P* times of five stations (*TT*, *CZ*, *KY*, *MZ* and *OY*) indicate that the *P*

velocity of the upper crust should be about 6.0 km/s rather than 5.8 km/s. (3) Lateral heterogeneity of the upper crust was made clear by the travel time analysis. For the events of the western Shikano and the Misasa regions P times delay by about 0.2 sec at MZ as compared to calculated ones for the velocity 6.0 km/s. (4) Apparent V_p/V_s values in various regions range from 1.66 to 1.71 (5) The Conrad discontinuity has a depth of 16 km beneath the Tottori region and 22 km beneath the Chizu and Ohara regions according to the analyses of SxS phases, dipping southward at an angle larger than 10°. (6) From SxS phases the depths of the nearby microearthquakes with S–P times less than or equal to 1.5 sec observed at TT are estimated to be confined to the following two ranges; 0–2 km and 4–8 km. (7) The SxP phases are found for the swarm of April, 1973, Misasa. (8) In the Hamasaka region there are very shallow events accompanied by SP phases. (9) The oscillatory waves which appear just after P waves and of which amplitudes are predominant in the radial component would be interpreted as channel waves of SP type propagated through the superficial layer. (10) A peculiar later phase having a considerably larger transversal component was observed for the shallow shock of October 18, 1972, Chizu (M3.3). This phase arrived just after the P wave and cannot be explained as an SH wave. This nature may be due to the lateral heterogeneity of the uppermost part of the crust.

Acknowledgements

The author wishes to express his sincere thanks to Professors Yoshimichi Kishimoto and Kazuo Oike for their valuable suggestions in the study of microearthquakes, Messrs Sei Yabe and Setsuro Nakao for their various aids in data processing, and Mrs. Mitsuko Koga for her kind help in reading the seismograms. The expense of the present study was defrayed by Grant in Aid for Scientific Research, the Ministry of Education of Japan.

References

1) Kishimoto, Y. and M. Hashizume: On the mechanism of earthquake swarm at Hamasaka, Bull. Disas. Prev. Res. Inst., Kyoto Univ., Vol. 16, Part 1, 1966, pp. 41–55.
2) Hashizume, M., K. Oike and Y. Kishimoto: Investigation of microearthquakes in Kinki District-seismicity and mechanism of their occurence-, Bull. Disas. Prev. Res. Inst., Kyoto Univ., Vol. 15, Part 3, 1966, pp. 35–47.
3) Hashizume, M.: Investigation of microearthquakes-On seismicity-Bull. Disas. Prev. Res. Inst., Kyoto Univ., Vol. 19, Part 2, No. 159, 1969, pp. 67–85.
4) Hashizume, M.: Investigation of microearthquakes-On the nature of the crust-, Bull. Disas. Prev. Res. Inst., Kyoto Univ., Vol. 20, Part 2, 1970, pp. 1–12.
5) Hashizume, M.: Investigation of microearthquakes-On earthquake occurrence in the crust-, Bull. Disas. Prev. Res. Inst., Kyoto Univ., Vol. 20, Part 2, 1970, pp. 65–94.
6) Nishida, R.: Activity of earthquakes occurred in April 1970 near Funaoka station, Disas. Prev. Res. Inst. Annuals, Kyoto Univ., No. 14A, 1971, pp. 165–175 (in Japanese).
7) Kishimoto, Y. and R. Nishida: Mechanisms of microearthquakes and their relation to geological structures, Bull. Disas. Prev. Res. Inst., Kyoto Univ., Vol. 23, Part 1, 1973,

pp. 1–25.
8) Huzita, K., Y. Kishimoto and K. Shiono: Neotectonics and seismicity in the Kinki Area, southwest Japan, Jour. Geosci. Osaka City Univ., Vol. 16, 1973, pp. 93–124.
9) Tottori Microearthquake Observatory: Recent seismicity of Microearthquakes in eastern Chugoku and northern Kinki districts, Disas. Prev. Res. Inst. Annuals, Kyoto Univ., No. 16B, 1973, pp. 65–76 (in Japanese).
10) Nishida, R.: Earthquake generating stress in eastern Chugoku and northern Kinki districts, southwest Japan, Bull. Disas. Prev. Res. Inst., Kyoto Univ., Vol. 22, Part 3, 1973, pp. 197–233.
11) Oike, K.: On a list of hypocenters compiled by the Tottori Microearthquake Observatory, Zisin, Vol. 28, No. 3, 1975, pp. 331–346 (in Japanese).
12) Nishida, R., S. Nakao and S. Yabe: Seismicity of San'in district, Disas. Prev. Res. Inst. Annuals, Kyoto Univ., No. 17B, 1973, pp. 69–81 (in Japanese).
13) Tsukuda, T., S. Nakao and Y. Kishimoto: Recent seismicity of the Tottori area, Disas. Prev. Res. Inst. Annuals, Kyoto Univ., No. 19B, 1976 (in preparation).
14) Omote, S.: Aftershocks that accompanied the Tottori Earthquake of Sept. 10, 1943, Bull. earthq. Res. Inst., Vol. 33, 1955, pp. 641–661.
15) The Research Group for Explosion Seismology: Crustal structure in the western part of Japan derived from the observation of the first and second Kurayoshi and the Hanabusa explosions, Part 1. observation of seismic waves generated by the first and second Kurayoshi and the Hanabusa explosions, Bull. Earthq. Res. Inst., Vol. 44, 1966, pp. 89–107.
16) Hashizume, M., O. Kawamoto, S. Asano, I. Muramatu, T. Asada, I. Tamaki and S. Murauchi: Crustal structure in the western part of Japan derived from the observation of the first and second Kurayoshi and the Hanabusa explosions, Part 2. crustal structure in the western part of Japan, Bull. Earthq. Res. Inst., Vol. 44, 1966, pp. 109–120.
17) Mino, K., R. Nishida and J. Miyakoshi: On temporary observation of microearthquakes near Tottori city (I), Disas. Prev. Res. Inst. Annuals, Kyoto Univ., No. 14A, 1971, pp. 177–188 (in Japanese).
18) Mizoue, M.: Crustal structure from travel times of reflected and refracted seismic waves recorded at Wakayama Microearthqiake Observatory and its substations, Bull. Earthq. Res. Inst., Vol. 49, 1971, pp. 33–62.
19) Kamitsuki, A.: On seismic waves reflected at the Mohorovičić discontinuity (1), Mem. Coll. Sci. Univ. Kyoto, Ser. A., Vol. 28, 1956, pp. 143–159.
20) Sanford, A.R. and L.T. Long: Microearthquake crustal reflections, Socorro, New Mexico, Bull. Seism. Soc. Amer., Vol. 55, 1965, pp. 579–586.
21) Sanford, A. R., Ö. Alptekin and T.R. Toppozada: Use of reflection phases on microearthquake seismograms to map an unusual discontinuity beneath the Rio Grande Rift, Bull. Seism. Soc. Am., Vol. 63, No. 6, 1973, pp. 2021–2034.
22) Kawasaki, I., Y. Suzuki and R, Sato: Seismic waves due to a shear fault in a semi-infinite medium: Part I, J. Phys. Earth, Vol. 21, 1973, pp. 251–283; Part II, J. Phys. Earth, Vol. 23, 1975, pp. 43–61.

Appendix 1

Hypocenter determination for P times of four stations:

We want to determine the four source parameters x, u, h and t, where x, y and h are coordinates of a focus and t is origin time. Let us assume that the medium is a homogeneous semi-infinite space and stations are located at the free surface. The source parameters which statisfy the P arrival times of stations A, B and C should describe a curve in the three dimensional space (x, y, h) for a parameter t. The

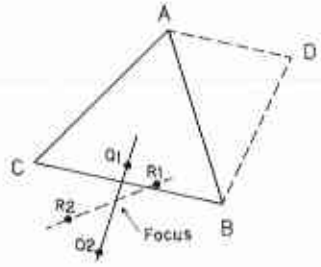

Fig. 25. Illustration of hypocenter determination for four stations.

curve passes Q_1 for $t=t_1$ and Q_2 for $t=t_2$ (Fig. 25). Assume that the difference between t_1 and t_2 is small enough for us to be able to regard the curve as a straight line. In a similar manner we can obtain R_1 and R_2 for stations A, B and D. The intersection of Q_1Q_2 and R_1R_2 is the focus determined.

Q_1 is obtained as the intersection of the three spheres with radii r_A, r_B and r_C respectively where,

$$\begin{aligned} r_A &= V_0(t_A - t) \\ r_B &= V_0(t_B - t) \\ r_C &= V_0(t_C - t) \end{aligned} \qquad (9)$$

V: P velocity of the medium,
t_A etc.: arrival time at A etc..

Q_2, R_1 and R_2 are obtained similarly.

The values of t_1 and t_2 should be selected by trial and error. In most cases of the present study the difference between t_1 and t_2 is taken as 0.1 sec.

Hypocenter determination for P times and S–P times of three stations:

In this case origin time is determined by Eq. (1) in Section 6. Then the focus is obtained in the same way as we obtain Q_1 etc. . In the present study when α in Eq. (1) is larger than 1.5 and smaller than 1.4 we fix the value as 1.5 and 1.4 respectively.

Appendix 2

Table 6. List of events used for hypocenter location and V_p/V_s determination.
The notations are as follows:
PS time : *S–P* time.
PF time : *F–P* time or the duration time of oscillation.
Mag. : *PF* time magnitude defined as $M=2.97 \log_{10} PF\ (in\ sec.)-2.55$[11].
α : See Eq. (1).
T, *C*, *K* etc. : *TT*, *CZ*, *KY* etc.,

No.	Date	Origin Time h m s	*PS* Time at *TT* (sec)	*PF* Time at *TT* (sec)	*Mag.*	α	V_p/V_s	Stations for V_p/V_s	Hypocentral Coordinates (km) x y h	*P* Velocity (km/sec)	Stations for Hypocenter Determination	Angle of Incidence of *P* at *TT* (°)
					Kurayoshi 5.1 sec≦*PS*≦6.6 sec							
1	Mar. 15, 1973	16 36	5.3	20	1.3	1.67	1.60	C T				
2	Aug. 12, 1974	02 17 11.1	5.5	15	0.9	1.53	1.65	K T M	−34.5 −29.8 13.6 −36.1 −29.3 15.9	5.8 6.0	K T M	
3	Oct. 25, 1974	03 32 08.6	5.5	30	1.8				−34.4 −30.1 13.2 −36.1 −29.6 15.5	5.8 6.0	K T M	24.3
4	Nov. 15, 1974	07 20 10.7	5.6	20	1.3	1.59	1.63	K T M	−46.2 −12.1 11.1 −48.6 −10.4 9.8	5.8 6.0	K T M	
5	Dec. 27, 1974	11 03 38.9	5.9	35	2.0	1.56	1.64	K T	−48.7 −17.2 (0.0) −51.3 −15.9 (0.0)	5.8 6.0	K T M	
6	Feb. 14, 1975	16 28 52.5	5.1	40	2.2				−41.8 −10.2 4.4 −43.6 −9.7 1.3	5.8 6.0	K T C	
7	May 01, 1975	01 02 24.4	6.3	13	0.8	1.51	1.66	K T				
8	May 16, 1975	10 41 49.5	6.6	12	0.7	1.49	1.67	K S T	−46.6 −8.8 9.7 −48.3 −10.6 8.2	5.8 6.0	K S T	
9	May 16, 1975	10 48 16.4	6.6	15	0.9	1.41	1.71	K S T C	−50.3 −18.1 13.4 −52.8 −18.1 11.8	5.8 6.0	K T C	
10	Nov. 11, 1975	04 50 54.3	6.2	20	1.3	1.29	1.78	K S T	−42.2 −20.8 8.8 −43.5 −23.5 2.4	5.8 6.0	K S T	
11	Nov. 19, 1975	14 19 26.5	5.9	20	1.3	1.43	1.70	K S T	−46.8 −9.5 11.1 −48.4 −11.4 9.8	5.8 6.0	K S T	
12	Dec. 14, 1975	20 20 08.9	6.0	20	1.3	1.43	1.70	K S T	−45.6 −11.7 16.0 −47.1 −13.7 15.2	5.8 6.0	K S T	

No.	Date	Origin Time h m s	*PS* Time at *TT* (sec)	*PF* Time at *TT* (sec)	*Mag.*	α	V_p/V_s	Stations for V_p/V_s	Hypocentral Coordinates (km) x y h	*P* Velocity (km/sec)	Stations for Hypocenter Determination	Angle of Incidence of *P* at *TT* (°)
				Kurayoshi 4.3 sec≦*PS*≦5.0 sec								
1	Jan. 13, 1973	21 05 37.2	5.0	100	3.4	1.39	1.72	K T C	−41.2 −16.0 14.3	5.8	K T C M	
		38.1							−38.5 −15.8 9.2	6.0		
2	Jan. 13, 1973	21 09 57.8	5.0	30	1.8	1.43	1.70	K T C	−41.9 −16.2 14.8	5.8	K T C M	
		58.7							−39.2 −15.9 10.3	6.0		
3	Jan. 13, 1973	21 23 57.7	5.0	30	1.8	1.51	1.66	K T C	−37.6 −16.0 9.9	5.8	K T C M	
		58.5							−35.6 −15.8 (0.0)	6.0		
4	Jan. 14, 1973	02 58 10.6	5.0	15	0.9	1.51	1.66	K T C	−39.0 −15.1 11.9	5.8	K T C	
									−40.7 −14.9 12.1	6.0		
5	Jan. 22, 1973	19 52 04.4		110	3.5				−41.7 −15.4 14.7	5.8	K T C M	
		05.3							−38.8 −15.3 9.5	6.0		
6	Jan. 22, 1973	20 37	5.0	12	0.7	1.55	1.65	T C				
7	Jan. 22, 1973	20 41 51.5	5.0	10	0.4	1.52	1.66	K T C	−39.2 −15.8 11.5	5.8	K T C	
									−40.9 −15.7 11.6	6.0		
8	Jan. 23, 1973	11 05 03.8	5.0	20	1.3	1.50	1.67	K T C	−40.9 −15.5 13.2	5.8	K T C M	
		04.8							−36.2 −15.0 12.8	6.0		
9	Feb. 08, 1973	20 21 23.4	5.0	15	0.9	1.35	1.74	T C M O	−46.6 −13.8 19.9	5.8	K T C M	
		24.4							−43.9 −13.7 14.9	6.0		
10	Apr. 01, 1973	23 33 44.3	4.4	20	1.3	1.41	1.71	T C M O	−29.3 −9.6 18.6	5.8	T C M O	
		45.1							−28.4 −9.9 12.4	6.0		
11	Jul. 08, 1973	07 56 57.0	5.0	20	1.3	1.32	1.76	K T C	−39.6 −10.2 5.3	5.8	K T C	
									−41.3 −9.8 4.5	6.0		
12	Jul. 15, 1973	02 47 37.8	4.4	20	1.3	1.51	1.66	K T C	−31.0 −15.6 6.4	5.8	K T C M	
		38.5							−30.4 −15.7 (0.0)	6.0		
13	Sep. 20, 1973	07 16 01.5	4.8	20	1.3	1.50	1.67	K T C	−38.7 −18.0 9.8	5.8	K T C M	
		02.2							−38.3 −18.0 (0.0)	6.0		
14	Apr. 29, 1974	00 09 49.3	4.7	20	1.3	1.42	1.70	K T C	−36.9 −11.0 8.3	5.8	K T C	
									−38.4 −10.6 8.5	6.0		
15	May 03, 1974	10 00 42.0	4.7	20	1.3	1.45	1.69	K T C	−37.7 −10.9 7.6	5.8	K T C	
									−39.7 −11.4 7.2	6.0		
16	Feb. 21, 1975	08 10 12.4	4.4	40	2.2	1.58	1.63	K T M	−35.4 −16.3 6.5	5.8	K T M	
									−37.1 −15.0 8.5	6.0		

17	Apr.	08, 1975	01 20 03.6	4.5	13	0.7	1.41	1.71	K T C	−35.7 −8.1 4.5 −37.1 −7.4 4.7	5.8 6.0	K T C	
18	Jul.	21, 1975	14 21 44.6 44.9	4.3	20	1.3	1.54	1.65	K S T C	−31.1 −16.4 4.4 −31.1 −16.4 (0.0)	5.8 6.0	K S T C	
19	Sep.	04, 1975	03 49 34.3	4.3	14	0.9	1.53	1.65	K S T	−32.3 −20.3 4.4 −33.3 −22.9 (0.0)	5.8 6.0	K S T	
20	Nov.	05, 1975	01 11 58.2	4.7	12	0.7	1.64	1.61	K T	−39.8 −13.9 11.7 −41.0 −16.1 10.6	5.8 6.0	K S T	
21	Nov.	20, 1975	10 26 33.4 34.1	4.8	17	1.1	1.57	1.64	K S T	−42.4 −15.2 15.2 −40.6 −14.9 11.5	5.8 6.0	K S T M	
						Misasa 3.3 sec≤*PS*≤4.0 sec							
1	Feb.	02, 1973	18 58 16.1	3.4	15	0.9	1.46	1.68	K T C	−26.0 −9.4 10.6 −26.8 −8.8 12.0	5.8 6.0	K T C	
2	Apr.	22, 1973	04 37 53.5	3.7	15	0.9	1.45	1.69	K T C	−29.0 −9.2 6.1 −30.0 −8.6 7.7	5.8 6.0	K T C	35.3
3	Apr.	22, 1973	15 20 18.5	3.8	15	0.9	1.48	1.68	K T C	−29.6 −8.4 8.5 −30.6 −7.8 9.7	5.8 6.0	K T C	
4	Apr.	23, 1973	02 42 26.3	3.7	20	1.3	1.38	1.72	K T C	−28.2 −10.2 0.7 −29.1 −9.7 4.7	5.8 6.0	K T C	13.3
5	Apr.	23, 1973	10 30 07.3 08.9	3.8	40	2.2	1.35	1.74	K T C	−37.5 −7.0 23.3 −32.9 −8.0 14.0	5.8 6.0	K T C O	22.3
6	Apr.	23, 1973	13 01	3.8	15	0.9	1.75	1.57	T C				38.3
7	Apr.	24, 1973	15 15 47.4 49.0	3.8	30	1.8	1.47	1.68	K T C	−36.4 −6.5 20.9 −31.7 −7.6 10.8	5.8 6.0	K T C O	
8	Apr.	24, 1973	15 17 13.7 15.3	3.7	40	2.2	1.52	1.66	T C	−34.4 −7.8 18.0 −29.7 −8.8 6.6	5.8 6.0	K T C O	23.6
9	May	01, 1973	05 51	3.8	15	0.9	1.40	1.71	K T				
10	May	01, 1973	06 58	3.8	12	0.7	1.47	1.68	K T				
11	Jul.	10, 1974	14 41 42.9	4.0	30	1.8	1.37	1.73	K T	−29.8 −10.0 5.9 −31.1 −8.2 7.8	5.8 6.0	K T M	
12	Jul.	17, 1974	05 12 50.7 52.2	3.9	20	1.3	1.35	1.74	K T C	−34.4 −5.6 17.9 −30.0 −6.9 6.8	5.8 6.0	K T C O	
13	Oct.	25, 1974	20 53	3.3	10	0.4	1.39	1.72	K T				
14	Aug.	13, 1975	15 36 36.9	3.8	20	1.3	1.42	1.70	S K T	−26.9 −8.2 12.8 −27.2 −9.9 13.6	5.8 6.0	S K T	
15	Sep.	04, 1975	05 40 46.6	3.5	10	0.4	1.46	1.68	S K T	−26.6 −9.0 11.1 −26.9 −10.8 11.8	5.8 6.0	S K T	

No.	Date	Origin Time h m s	*PS* Time at *TT* (sec)	*PF* Time at *TT* (sec)	*Mag.*	α	V_p/V_s	Stations for V_p/V_s	Hypocentral Coordinates (km) x y h	*P* Velocity (km/sec)	Stations for Hypocenrer Determination	Angle of Incidence of *P* at *TT* (°)
16	Sep. 21, 1975	19 55 16.6	4.0	40	2.2	1.55	1.65	K T	−30.2 −11.8 8.2	5.8	K S T M	19.5
		16.8							−30.5 −10.6 7.4	6.0		
17	Dec. 02, 1975	05 53	3.5	10	0.4	1.77	1.56	K T				
					Shikano		2.7 sec≤*PS*≤3.2 sec					
1	Feb. 05, 1973	13 30 10.3	2 8	15	0.9	1.57	1.64	K T C	−20.2 −8.0 11.9	5.8	K T C	
									−20.6 −7.3 13.4	6.0		
2	Mar. 19, 1973	07 54 15.8	2.9	45	2.4	1.45	1.69	T O M	−17.7 −5.1 15.1	5.8	T O M	
									−19.6 −3.4 14.5	6.0		
3	Apr. 12, 1973	17 33 30.6	3.1	40	2.2	1.39	1.72	T C O M	−23.0 −9.2 19.4	5.8	K T C O	
		31.3							−22.3 −9.6 14.7	6.0		
4	Apr. 13, 1973	16 36 14.9	3.0	12	0.7	1.60	1.63	T C				
5	Apr. 17, 1973	15 49 50.8	3.0	20	1.3	1.44	1.69	T C O M	−22.0 −10.7 17.8	5.8	K T C O	35.3
		51.6							−21.3 −11.2 11.1	6.0		
6	Jul. 22, 1974	07 32 41.8	2.7	70	2.9	1.37	1.73	T C M	−20.3 −7.5 17.3	5.8	K T C O	
		42.4							−20.1 −7.9 12.8	6.0		
7	Sep. 28, 1974	20 51 30.1	3.2	15	0.9	1.29	1.78	K T C	−22.1 −14.6 3.4	5.8	K T C	
									−22.6 −14.4 6.8	6.0		
8	Oct. 09, 1974	23 20 04.5	2.8	20	1.3	1.45	1.69	K T C M	−19.1 −9.4 6.6	5.8	K T C M	
		05.2							−19.2 −10.0 (0.0)	6.0		
9	Oct. 21, 1975	10 03	2.8	10	0.4	1.32	1.76	S T				
					Shikano		2.2 sec≤*PS*≤2.5 sec					
1	Nov. 11, 1973	06 45 26.7	2.3	25	1.6	1.93	1.52	T K C	−13.1 −6.2 13.3	5.8	T K C O	
		27.2							−13.2 −6.7 9.7	6.0		
2	Feb. 07, 1974	04 29 03.0		150	3.9				−14.8 −6.8 15.3	5.8	T K C O	
		03.5							−14.8 −7.3 11.5	6.0		
3	Feb. 07, 1974	04 29 48.1	2.2	30	1.8	1.27	1.79	T C				
4	Feb. 07, 1974	04 30 23.2	2.5	30	1.8	1.32	1.76	T K	−15.3 −6.3 15.4	5.8	T K C O	
		23.7							−15.5 −6.8 11.5	6.0		
5	Dec. 01, 1974	17 27 38.4	2.2	15	0.9	1.56	1.64	T K M	−15.6 −6.0 9.4	5.8	T K M	
									−15.9 −3.9 11.2	6.0		

6	Jul.	03, 1975	14 58	25.4 25.7	2.5	20	1.3	1.53	1.65	TCOM	−8.8 −8.6	−9.4 −8.9	3.6 (0.0)	5.8 6.0	TCOM
7	Jul.	07, 1975	11 18	07.9 08.1	2.4	25	1.8	1.59	1.63	TKC	−16.5 −16.6	−7.2 −7.1	6.4 5.6	5.8 6.0	STKC
8	Jul.	18, 1975	15 47	46.4	2.3	15	0.9	1.62	1.62	STC	−15.6 −16.3	−5.0 −4.3	9.4 9.7	5.8 6.0	STC
9	Nov.	14, 1975	16 36	37.2 37.4	2.4	20	1.3	1.50	1.67	STCOM	−15.9 −16.1	−6.9 −6.6	7.4 6.6	5.8 6.0	STKC
							Yoshioka 1.4 sec≤*PS*≤2.1 sec								
1	Jan.	13, 1973	02 37	45.7	1.8	10	0.4	1.51	1.66	TCK	−9.3 −8.9	−5.2 −4.4	11.5 12.8	5.8 6.0	TCK
2	Mar.	13, 1973	07 56	40.8	1.9	20	1.3	1.47	1.68	TCK	−10.0 −9.5	−5.6 −4.8	10.8 12.2	5.8 6.0	TCK
3	Jul.	27, 1973	06 37	16.9 17.2	1.4	25	1.6	1.42	1.70	TCOM	−6.5 −6.5	−2.5 −2.7	12.1 10.4	5.8 6.0	TCKO
4	Feb.	16, 1975	22 37	15.0	2.1	10	0.4	1.73	1.58	TKC	−12.9 −12.7	−4.9 −4.0	11.6 13.0	5.8 6.0	TKC
5	Aug.	27, 1975	11 54	52.2 52.4	1.5	35	2.0	1.50	1.67	TSCK	−7.7 −7.7	−4.8 −5.0	5.7 2.8	5.8 6.0	TSCK
6	Sep.	20, 1975	03 29	38.2	1.5	15	0.9	1.55	1.65	TSC	−5.8 −5.9	−5.1 −4.4	10.2 11.0	5.8 6.0	TSC
7	Oct.	10, 1975	23 55		1.5	25	1.6	1.32	1.76	TS					
8	Oct.	24, 1975	08 27		1.5	15	0.9	1.42	1.70	TS					
9	Nov.	12, 1975	12 11		1.5	12	0.7	1.64	1.61	TS					
10	Nov.	12, 1975	13 04	53.9 54.3	1.4	25	1.6	1.42	1.70	TCOM	−8.4 −7.5	−3.6 −4.0	8.9 6.7	5.8 6.0	TSCO
							Tottori 1.4 sec≤*PS*≤2.0 sec								
1	Sep.	18, 1973	20 44	22.2 22.5		120	3.6				0.5 0.4	−9.3 −9.6	6.9 3.5	5.8 6.0	TCKO
2	Sep.	23, 1973	09 34	07.4 07.8	1.4	30	1.8	1.35	1.74	TCK	0.4 0.5	−9.1 −9.4	7.2 3.0	5.8 6.0	TCKO
3	Sep.	23, 1973	12 24	16.0 16.3	1.4	20	1.3	1.60	1.63	TCK	−1.0 −0.9	−8.8 −9.0	6.6 3.1	5.8 6.0	TCKO
4	Nov.	07, 1973	19 51	34.6 34.9	2.0	25	1.6	1.40	1.71	TOKM	13.4 13.9	−1.9 −2.0	9.0 5.3	5.8 6.0	TCOK

No.	Date	Origin Time h m s	*PS* Time at *TT* (sec)	*PF* Time at *TT* (sec)	*Mag.*	α	V_p/V_s	Stations for V_p/V_s	Hypocentral Coordinates (km) x	y	h	*P* Velocity (km/sec)	Stations for Hypocenter Determination	Angle of Incidence of *P* at *TT* (°)
5	Jan. 04, 1974	21 23 09.6	1.5	30	1.8	1.42	1.70	T O M	8.6	0.5	11.0	5.8	T C O K	
		10.0							8.5	−0.1	8.5	6.0		
6	Feb. 17, 1974	04 16 57.8	1.4	25	1.6	1.42	1.70	T C O K M	4.7	−3.7	10.6	5.8	T C O K	
		58.1							4.6	−4.0	8.9	6.0		
7	Aug. 09, 1975	14 02 37.8	1.4	40	2.2	1.49	1.67	T S O M	2.0	−5.1	10.9	5.8	T S O M	
		37.9							1.7	−3.8	11.3	6.0		
8	Oct. 10, 1975	09 00	1.4	20	1.3	1.43	1.70	T M						
9	Oct. 10, 1975	19 38 17.8	1.5	15	0.9	1.46	1.68	T S M	6.2	−1.7	10.4	5.8	T S M	
									6.3	0.3	10.9	6.0		
					Hamasaka 2.6 sec≤*PS*≤4.5 sec									
1	Oct. 17, 1971	17 38 40.0	3.3	40	2.2	1.42	1.70	O T M I	27.0	2.6	11.7	5.8	O T M I	30.5
		40.6							25.9	2.2	2.0	6.0		
2	Oct. 17, 1971	18 52 04.5	3.4	55	2.6	1.41	1.71	O T M I	27.0	2.6	11.7	5.8	O T M I	40.8
		05.1							25.9	2.2	2.0	6.0		
3	Oct. 17, 1971	18 53 13.6	3.3	50	2.5	1.40	1.71	O T M I	27.1	2.1	11.6	5.8	O T M I	41.3
		14.2							26.8	1.8	2.0	6.0		
4	Oct. 17, 1971	21 27 43.6	3.3	25	1.6	1.43	1.70	O T M I	27.3	3.0	13.0	5.8	O T M I	35.8
		44.2							27.1	2.6	5.5	6.0		
5	Mar. 23, 1973	20 47 16.9	3.2	25	1.6	1.42	1.70	O T C M I	26.7	−6.6	15.3	5.8	O T C M	
		17.3							26.6	−6.5	12.0	6.0		
6	Apr. 28, 1973	23 47 27.2	3.4	45	2.4	1.38	1.72	T O M I	29.0	7.4	14.7	5.8	T O M I	
		27.8							28.8	7.1	7.3	6.0		
7	May 04, 1973	02 27 09.0	3.3	20	1.3	1.44	1.69	T O M I	27.6	6.5	17.1	5.8	T O M I	
		09.6							27.4	6.2	11.1	6.0		
8	May 07, 1973	07 48 19.4	3.4	25	1.6	1.48	1.68	T O C M I	26.6	3.2	(0.0)	5.8	T O C M	
		20.1							25.9	2.2	(0.0)	6.0		
9	Jun. 27, 1973	08 02 03.7	3.2	20	1.3	1.46	1.68	O T C I	25.7	0.1	8.3	5.8	O T C M	
		04.4							25.7	−0.5	(0.0)	6.0		
10	Jun. 30, 1973	04 13 19.5	3.5	35	2.0	1.39	1.72	O T C M K	29.3	1.3	9.1	5.8	O T C M	40.0
		20.2							28.6	0.7	(0.0)	6.0		
11	Sep. 25, 1973	07 38 18.1	2.7	12	0.7	1.49	1.67	C T O M I	18.6	−12.5	7.9	5.8	C T O M	
		18.5							18.5	−12.5	1.3	6.0		

12	Mar.	04, 1974	01	23	32.4	3.0	30	1.8	1.51	1.66	TOCKI	23.9	−0.9	8.1	5.8	TOCM	
					33.1							23.6	−1.5	(0.0)	6.0		
13	Aug.	25, 1974	10	41	27.5	4.4	35	2.0	1.40	1.71	OTCMI	33.8	13.2	12.4	5.8	OTCM	
					28.4							33.0	11.8	(0.0)	6.0		
14	Sep.	30, 1974	20	05	27.7	2.6	40	2.2	1.37	1.73	TKMH	20.1	1.5	4.3	5.8	TKMH	
					28.1							20.0	1.6	(0.0)	6.0		
15	May	23, 1975	20	48	59.5	3.4	30	1.8	1.44	1.69	OTCSHI	27.9	0.0	14.3	5.8	OTCS	
					60.1							27.5	−0.3	9.5	6.0		
16	May	30, 1975	10	10	14.9	3.4	50	2.5	1.39	1.72	OTCSHI	26.8	−1.8	14.1	5.8	OTCS	
					15.3							26.9	−1.9	9.9	6.0		
17	Sep.	09, 1975	12	53	05.4	3.4	17	1.1	1.50	1.67	TCS	27.3	6.9	9.1	5.8	TCS	
												29.5	8.4	(0.0)	6.0		
18	Nov.	03, 1975	08	07	21.4	4.5	35	2.0	1.54	1.65	OTSMI	34.0	13.7	14.2	5.8	OTSM	
					21.6							35.1	15.5	7.7	6.0		
											Hamasaka 5.4 sec≤*PS*≤6.3 sec						
1	May	07, 1973	05	38	01.0	6.3	15	0.9	1.39	1.72	OTCIM	49.2	5.4	19.4	5.8	OTCM	
					01.8							48.4	5.1	13.8	6.0		
2	Sep.	25, 1975	10	38	13.8	5.4	17	1.1	1.47	1.68	OHCTI	42.4	−14.1	6.5	5.8	OCTI	
					14.2							41.8	−14.6	4.2	6.0		
3	Nov.	24, 1975	00	58	50.7	6.3	50	2.5	1.45	1.69	OTCIM	52.1	13.5	20.2	5.8	OTCI	
					51.3							52.3	14.0	13.9	6.0		
4	Nov.	24, 1975	01	38	53.5	6.3	50	2.5	1.46	1.68	OHTCIM	51.8	13.9	22.2	5.8	OTCI	
					54.1							51.7	14.0	16.8	6.0		
											Chizu 2.5 sec≤*PS*≤3.5 sec						
1	Sep.	14, 1972	05	13	36.0	3.5	12	0.7	1.40	1.71	TOI	0.8	−27.0	8.9	5.8	CTO	
												−0.5	−28.1	8.5	6.0		
2	Nov.	24, 1972	21	10	26.8	2.7	20	1.3	1.36	1.74	CTOK	2.1	−21.5	6.7	5.8	CTOK	
					27.1							2.2	−21.1	3.9	6.0		
3	Oct.	03, 1974	20	25	42.5	2.6	35	2.0	1.49	1.67	TKM	2.8	−18.9	12.0	5.8	TKM	36.1
												4.1	−19.1	12.9	6.0		
4	Jul.	11, 1975	01	15	48.8	2.6	15	0.9	1.54	1.65	CTSO	3.0	−22.8	7.4	5.8	CTSO	39.8
					50.1							2.9	−22.6	5.5	6.0		
5	Aug.	03, 1975	00	03	03.2	3.1	25	1.6	1.38	1.72	CTMO	−0.4	−24.4	6.7	5.8	CTMO	
					03.5							−0.6	−24.3	4.5	6.0		
6	Sep.	16, 1975	01	33	25.2	2.5	15	0.9	1.43	1.70	CTKO	−1.2	−20.5	7.1	5.8	CTKO	
					25.5							−1.2	−20.3	4.0	6.0		

No.	Date	Origin Time h m s	*PS* Time at *TT* (sec)	*PF* Time at *TT* (sec)	*Mag.*	α	V_p/V_s	Stations for V_p/V_s	Hypocentral Coordinates (km) x y h	*P* Velocity (km/sec)	Stations for Hypocenter Determination	Angle of Incidence of *P* at *TT* (°)
7	Nov. 26, 1975	18 50 21.6 21.9	2.7	25	1.6	1.38	1.72	C T S O K M	2.0 −22.4 9.4 1.8 −22.2 7.5	5.8 6.0	C T S O	
8	Dec. 05, 1975	12 43 26.2	2.9	15	0.9	1.44	1.69	C T O	5.1 −23.1 5.3 4.1 −24.0 6.1	5.8 6.0	C T O	
								Chizu 4.4 sec≤*PS*≤5.0 sec				
1	Oct. 18, 1972	06 02 04.5 04.7	4.5	90	3.3	1.46	1.68	M T O	−0.3 −36.2 5.3 −0.6 −36.3 (0.0)	5.8 6.0	C M T O	
2		16 23 24.5 24.7	4.5	20	1.3	1.61	1.62	C M T O	0.4 −35.9 2.5 0.2 −36.0 (0.0)	5.8 6.0	C M T O	
3		19 30 33.0 33.3	4.5	25	1.6	1.52	1.65	C M T O	−0.3 −36.3 2.7 −0.3 −36.4 (0.0)	5.8 6.0	C M T O	
4	Oct. 20, 1972	22 58 43.1 43.4	4.5	15	0.9	1.58	1.63	C M T O	−0.3 −36.2 5.0 −0.5 −36.4 (0.0)	5.8 6.0	C M T O	
5	Oct. 21, 1972	00 31 42.1 42.4	4.5	25	1.6	1.52	1.65	C M T O K	−0.3 −36.2 5.0 −0.5 −36.4 (0.0)	5.8 6.0	C M T O	
6	Dec. 13, 1972	12 31 57.9 58.1	4.4	35	2.0	1.40	1.71	C M T O	7.6 −34.7 5.3 7.7 −34.8 2.6	5.8 6.0	C M T O	
7	Sep. 28, 1973	14 00 03 6 04.0	5.0	25	1.6	1.42	1.70	C O T K I	2.1 −45.3 5.0 2.2 −45.3 (0.0)	5.8 6.0	C M T O	
								Ohara 5.3 sec≤*PS*≤5.4 sec				
1	Mar. 04, 1974	06 24 15.1 15.4	5.3	25	1.6	1.51	1.66	C M O T I K	11.9 −40.8 13.3 12.0 −40.8 10.8	5 8 6.0	C M O T	
2	Mar. 04, 1974	06 37 11.7 12.0	5.3	25	1.6	1.57	1.64	C M O T I K	12.0 −41 0 13 7 12.3 −41.0 11.2	5 8 6 0	C M O T	
3	Jun. 13, 1975	21 27 01.1 01.5	5.4	35	2.0	1.44	1.69	C M O T I K H	11.6 −41 4 16 1 11.7 −41.5 13 9	5 8 6 0	C M O T	
4	Jun. 13, 1975	21 27 42 8 43.2	5.4	60	2.7	1.36	1.74	C M O T I K H	11.4 −41 7 16 0 11.6 −41.6 13 6	5 8 6 0	C M O T	21 0
5	Jun. 14, 1975	10 44 49.5 49.9	5.3	40	2.2	1.42	1.70	C M O T I K H	11.4 −41 3 14 9 11.9 −41.1 12.4	5 8 6 0	C M O T	
6	Jun. 15, 1975	15 25 52.0	5.3	20	1.3	1.37	1.73	C T K	9.1 −40.3 14 2 10.8 −41.9 12.9	5 8 6.0	C T K	